BUOYANT SLOT JETS INTO STAGNANT OR FLOWING ENVIRONMENTS

by

Klas Cederwall

(on leave from
Chalmers Institute of Technology, Goteborg, Sweden)

Project Supervisor:

Norman H. Brooks

Funded by

Water Quality Office
Environmental Protection Agency

and

The Swedish Board for Technical Development (STU)

W. M. Keck Laboratory of Hydraulics and Water Resources
Division of Engineering and Applied Science
California Institute of Technology
Pasadena, California

Report No. KH-R-25

April 1971

ACKNOWLEDGMENTS

I would like to express my deep gratitude to Dr. Norman H. Brooks for many valuable discussions on the subject of this study. For construction of the laboratory equipment, I am much indebted to Mr. Elton F. Daly, Supervisor of the Laboratory, and his assistants, Mr. Carl A. Green and Mr. Robert L. Greenway. A warm thank you is extended to Mrs. Arvilla F. Krugh for typing this manuscript.

The writer has had a stipend paid by the Swedish Board for Technical Development (STU) during a temporary research appointment at the W. M. Keck Laboratory of Hydraulics and Water Resources, California Institute of Technology. The work has been supported by Research Grant No. 16070 DGY of the Water Quality Office, Environmental Protection Agency, entitled Dispersion in Hydrologic and Coastal Environments.

ABSTRACT

The diffusion following the release of a buoyant slot jet into a confined, uniformly flowing environment has been studied. A dimensionless analysis reveals the complexity of the problem; there are in general four governing dimensionless numbers. However, if the overall mixing and not the details of the process of diffusion is of importance, we can define basic flow regimes using a reduced number of parameters.

Experiments were conducted first with a horizontal, buoyant slot jet into stagnant, ambient fluid. Observed trajectories and centerline dilutions were in good agreement with existing theories. In addition, two sets of experiments were performed with a vertical and a horizontal buoyant slot jet issuing into a uniformly flowing stream. A two-layer flow analysis provided the rationale for a classification of flow regimes. It was found that the mechanism of upstream intrusion of jet effluent is characterized primarily by a gross densimetric Froude number based on the ambient flow velocity and the buoyancy flux from the source. However, the formation of an upstream wedge may be hampered due to the effect of initial flux of momentum in the downstream direction.

When the buoyant slot jet cannot entrain all the oncoming flow, while maintaining the typical jet or plume behavior, then the jet flow pattern breaks up and there is efficient mixing close to the source.

CONTENTS

CONTENTS (Continued)

LIST OF FIGURES

LIST OF FIGURES (Cont'd)

LIST OF FIGURES (Cont'd)

LIST OF TABLES

CHAPTER I

INTRODUCTION

The ultimate disposal of man-made wastes is a major environmental problem of today. Pollution of the receiving waters has to be controlled effectively and reduced to such a level as to preserve the delicate balance of the natural biological processes. This is true for all kinds of wastes for which there exists a threshold for pollution below which the effect on the environment can be overlooked and tolerated. The degree of treatment, the choice of outfall site as well as the design of the outfall structure must be carefully considered so that water quality requirements of the receiving water can be met.

The initial mixing of the discharged waste water is basically a problem of jet diffusion, whereas the subsequent dispersion and dilution is a more complex phenomenon, due to the multitude of significant parameters involved. The usual practice is to provide deep-water outfalls in the ocean with a multiple-port diffuser to produce high initial dilution of the sewage. Similarly, diffusers may be used for thermal waste discharge when a high rate of mixing is required close to the outfall structure.

The efficiency of the initial mixing process is directly related to the flux of momentum and buoyancy from the source and is generally gained by a relatively close port spacing. Hence, from a practical

point of view, two-dimensional jet and plume flows are of considerable interest. The present study analyzes the gross behavior of buoyant slot jets in stagnant and flowing environments.

CHAPTER II

FLOW CONFIGURATIONS

II-1 Basic Assumptions and Dimensional Analysis

Fig. 1 shows a sketch of the problem. Restricting the study to the two-dimensional case the basic assumptions are:

1. The ambient flow is uniform with a constant velocity over the full depth.
2. The source is a line source characterized by initial fluxes of mass, momentum and buoyancy.
3. Steady state situation.*

Hence, the following independent parameters define the problem:

For the source

volume flux	$q = u_j B$	(1)
kinematic momentum flux	$m = u_j^2 B$	(2)
buoyancy flux	$b = \frac{\Delta\rho}{\rho} g u_j B$	(3)
angle of injection	θ	

and for the ambient flow

velocity	u_a
depth	H

---

* Upstream injection of the jet effluent may generate a pulsating jet flow pattern. The present study will be limited to an angle of injection $\theta \leq 90^\circ$ – see fig. 1 – in which case steady state situation always can be accomplished.

where u_j is the jet velocity and B the jet width at the slot; $\Delta\rho$ is the density difference between the ambient fluid and the discharged effluent and ρ a reference density chosen as that of the ambient fluid; g is the constant of gravity. The viscosity is omitted since we assume fully turbulent jet flow conditions at large Reynolds number in the vicinity of the outfall. This study will be restricted to the region close to the outfall, and does not include mixing by the ambient turbulence away from the source.

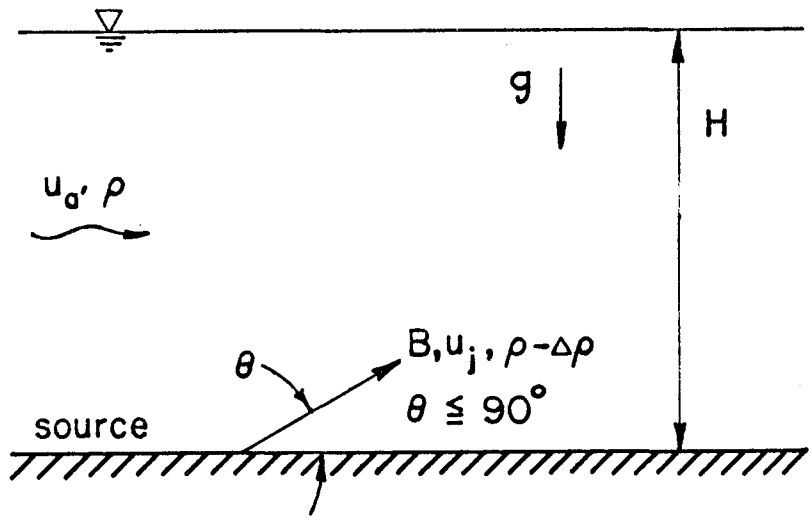

Fig. 1 Two-dimensional buoyant jet. Sketch of the problem.

The flow phenomenon is characterized by four dimensionless numbers chosen as

1. a velocity ratio

$$k = \frac{m}{q\, u_a} = \frac{u_j}{u_a} \tag{4}$$

2. a source Froude number

$$F = \frac{u_a^3}{b} = \frac{u_a^3}{q\frac{\Delta\rho}{\rho}g} \tag{5}$$

3. a volume flux ratio

$$V = \frac{u_a H}{q} \tag{6}$$

4. the angle of injection, θ.

II-2 Limiting Cases. *

From the dimensional analysis the flow regimes may be characterized by various dimensionless numbers as follows:

1. A buoyant slot jet in a confined, flowing environment, is defined by the four dimensionless numbers previously listed. However, there are certain limiting cases of interest. First, take the case of

2. A buoyant slot jet in an unconfined, flowing environment.

Let $H \to \infty$. Then V drops out as a governing parameter and we have left

k, F and θ

characterizing the problem.

3. A two-dimensional wall-jet in a confined region.

Let $b \to 0$; that is, density differences vanish. We are then left with

k, V and θ

as relevant parameters for the problem, neglecting the wall boundary layer.

4. A two-dimensional wall-jet in an unconfined region.

If in case 3, $H \to \infty$, V may be left out and we have only

k and θ

---

* See also Fig. 19.

5. A simple jet.

A simple jet of initial momentum flux only in a stagnant infinite environment has no governing flow parameter and is characterized by θ, the angle of injection, only. In case of a finite region $\frac{H}{B}$ is a scaling parameter.

6. A buoyant slot jet in a stagnant, confined region.

If $u_a \to 0$ the following three dimensionless parameters describe the problem,

the jet Froude number $F_j = F^{1/2}\, k^{3/2} = \dfrac{u_j}{\left(\frac{\Delta\rho}{\rho}\, g\, B\right)^{\frac{1}{2}}}$ (7)

a scaling ratio $\frac{H}{B}$

the angle of injection θ.

Now, let $H \to \infty$. This gives us

7. A buoyant slot jet in an unconfined, stagnant region, characterized by F_j and θ.

8. A simple, two-dimensional plume in a flowing environment.

For a simple plume $m \to 0$ and $q \to 0$,* that is, the source has both zero flux of momentum and zero mass flux. F is then the only governing parameter. If the region is finite, then H is a scaling length.

Finally we have

9. A simple plume in a stagnant environment.

For this case all the flow parameters drop out and we have H as a scaling length if the region is finite.

---

* If q does not go to zero along with m for a simple plume, b goes to infinity! This is a virtual (heat) source and the definition of b as given by Eq. (3) has no meaning; compare Eq. (30) and footnote.

II-3 Previous Studies.

A comprehensive survey of studies on jet and plume problems is given by Fan (1967). To supplement this review, some works more related to the present investigation have to be mentioned. Several recent papers have focused on the problem of axisymmetric jets and plumes in a cross flow (see Pratte and Baines (1967), Fan (1967), Platten and Keffer (1968) and Abraham (1970)); but there are few similar investigations for the two-dimensional case. An early paper by Rouse (1947) deals with gravitational diffusion from a boundary source in two-dimensional flow. The result of this study will be discussed in Chapter V. Rouse (1957) has also analyzed the process of diffusion in the lee of a two-dimensional jet in a cross-stream. Studies on reattached jets – wall jets – are frequently reported in the literature (see Rajaratnam and Subramanya (1968)). Sawyer (1963) investigated the effects of curvature on entrainment for two-dimensional wall jets.

Chapter IV of this report is an experimental study of a buoyant, horizontal slot jet in homogeneous and stagnant environment. This problem was first studied theoretically by Abraham (1963). Fan and Brooks (1969) extended the analysis to take an arbitrary angle of injection and also a linear density stratification of the ambient fluid. The general problem of a buoyant slot jet in a flowing, confined region is dealt with in Chapter V. The present findings can be compared to the result of a two-dimensional model study for the T. V. A. Browns Ferry Nuclear Power Plant (Harleman, Hall and Curtis, (1968)). The objective of this investigation was to find a diffuser design that would result in complete mixing between the heated condenser water and the ambient river flow.

CHAPTER III

APPLICATION TO PRACTICAL PROBLEMS

There are several environmental conditions that must be taken into consideration when analyzing problems of waste water disposal in lakes, rivers and in the ocean; the buoyancy effect arising from the density difference between the ambient water and the waste water, prevailing currents and density stratification of the waters in the disposal area are the most important ones. This study is restricted to a two-dimensional buoyant jet in a uniform, flowing or stagnant environment. Many situations of waste-water discharge may be approximately described by this case. The row of round jets from an outfall diffuser will — if the ports are closely spaced — gradually merge as they spread and at some distance from the diffuser behave like a two-dimensional jet. Uniform flow situations are often found in rivers, estuaries and coastal waters. In this chapter we will discuss the effect of jet interaction on the overall dilution of the waste discharged from a diffuser. The range of the governing flow parameters is estimated considering various waste disposal problems.

III-1 Jet Interference

Diffusers for ocean outfall pipes are sometimes designed so that interaction between the rising jets is avoided before the sewage field is established at the sea surface or at some neutrally buoyant level.

It is believed that jet interference would hamper the over-all rate of dilution between the discharged effluent and the ambient ocean water. Let us therefore first compare the mixing efficiency of a two-dimensional momentum jet and a row of round momentum jets. Assume that the volume and momentum fluxes per unit length are the same for both arrangements. This gives us the following relation:

$$B = n \frac{\pi D^2}{4} \tag{8}$$

where n is the number of ports per unit length of the diffuser, D the jet diameter of each individual port, and B the width of the jet from the slot.

The relative jet flow as a function of the distance, s, from the source may be written, Albertson, et al (1950), for a slot jet

$$\frac{Q}{Q_o} = 0.62 \left(\frac{s}{B}\right)^{\frac{1}{2}} \tag{9}$$

and for a three-dimensional jet

$$\frac{Q}{Q_o} = 0.32 \frac{s}{D} \tag{10}$$

To define when interaction occurs we have to assign a characteristic local width to the round jet. Let t be the nominal jet half-width, that is, the radius at the point where the local jet velocity equals $\frac{1}{e}$ of the centerline velocity. 2 t is then a measure of the local jet width and we may define interaction between the individual jets when

$$n \cdot 2t > 1 \tag{11}$$

A simple jet expands linearly with distance from the source. Applying the concept of entrainment for analyzing jet diffusion — see Fan (1967) and Fan and Brooks (1969) — we may express the growth of

the round jet by:

$$t = 2\alpha\, s \tag{12}$$

where α is the coefficient of entrainment. Experiments by Albertson et al. (1950), later confirmed by Ricou and Spalding (1961), give $\alpha = 0.057$ and we arrive at

$$2t = 0.228\, s \tag{13}$$

Hence, jet interference occurs when

$$ns > 4.4 \tag{14}$$

Let us compare the rate of dilution for the two outlet arrangements in the range where no interaction occurs. The ratio between these two dilutions is denoted by R and for $sn < 4.4$ we have

$$R = \frac{\left(\frac{Q}{Q_o}\right)_{\text{row of ports}}}{\left(\frac{Q}{Q_o}\right)_{\text{line source}}} = 0.45\,(sn)^{\frac{1}{2}} \tag{15}$$

At the point of interaction $sn = 4.4$ and $R = 0.95$. Hence, the over-all dilution produced by the jets will be practically the same for the two arrangements. The line source obviously entrains ambient fluid more effectively than the row of individual jets close to the source, that is when $sn < 4.4$.

Now, let us assume that the line source, as well as the row of point sources, is characterized by initial flux of buoyancy only. Using the result of Rouse et al. (1952), we may write the flow rate of the three-dimensional plume as

$$\frac{Q}{n} = 0.15\left(\frac{b}{n}\right)^{\frac{1}{3}} \cdot s^{5/3} \tag{16}$$

where b, as previously, denotes the buoyancy flux per unit length. Similarly, for the two-dimensional plume referring again to Rouse, et al. (1952) we get

$$Q = 0.57\, b^{\frac{1}{3}} s \tag{17}$$

Compare a row of point sources–n per length unit–with a line source, both arrangements having the same flux of buoyancy per length unit. As before, let us say that the plumes from the row of orifices interact when

$$n \cdot 2t > 1 \tag{18}$$

For a simple round plume, the plume half-width is found to be, Morton, et al. (1956)

$$t = \frac{6}{5}\alpha s \tag{19}$$

With the entrainment coefficient $\alpha = 0.082$ for this case, as indicated by the experiments of Rouse et al. (1952), we arrive at

$$n \cdot s > 5.1 \tag{20}$$

as a criterion for plume interaction. A ratio of dilutions R is defined as before:

$$R = \frac{\left(\frac{Q}{Q_o}\right) \text{row of ports}}{\left(\frac{Q}{Q_o}\right) \text{line source}} = 0.26\,(ns)^{2/3} \tag{21}$$

When the plumes from the diffuser start to interact, that is at a distance where $n \cdot s = 5.1$, we find that $R = 0.78$. This means that, for a given b-value, when the spacing of the ports is so close that the plumes actually interfere before reaching the sea surface or the level of submergence of the sewage field, then the rate of initial mixing will be increased. (Note that this is not an argument for a short diffuser vs. a longer one.)

A diffuser, however, is usually designed with horizontal ports along both sides of the pipe. In this case, interaction between the rising buoyant jets from the two rows of ports may significantly reduce the degree of initial mixing, see Fig. 2.

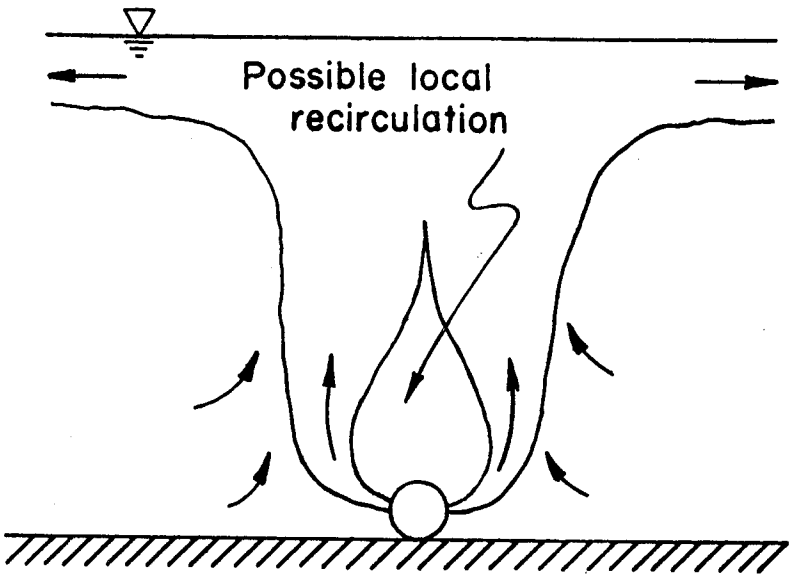

Fig. 2 Interaction between the rising buoyant jets of a diffuser.

Take the case of just one row of outlet ports along one of the diffuser sides as the reference case for comparison of the rate of initial mixing. Let us assume that the ports are so closely spaced that the mixing resembles that from a true line source. Obviously, this gives us the most efficient mixing for a given initial flux of buoyancy per unit length of the diffuser. Compare this case with a conventional diffuser arrangement having ports distributed on both sides of the pipe but with the same total flux of buoyancy per unit length of the diffuser. Assume that the mixing can be characterized by two non-interacting line sources of buoyancy only. From Eq. (17) it follows that this may increase the initial dilution by a factor $2^{2/3}$, that is roughly by 60%. On the other hand, if the plumes from the two line sources start interacting as they rise towards the sea surface, this may reduce the dilution of the sewage due to local recirculation, see Fig. 2, to be approximately equivalent to the reference case. Obviously, in a real situation

characterized also by initial flux of horizontal momentum some interaction may occur between the sewage jets from the two sides of the diffuser the over-all effect on the initial mixing depending on the flow parameters and the scaling of the flow field. Jet interference and related problems of diffuser design have recently been studied by Liseth (1970) at U. C. Berkeley.

III-2 Practical Problems

Two problems of waste water disposal will be discussed: discharge of heated cooling water into a river and marine disposal of sewage. In both cases we assume that the outfall facilities are equivalent to a single line source. If we have a uniformly flowing and homogeneous environment, then the present model of a buoyant slot jet applies. The two situations chosen cover a very wide range in the governing parameters.

A. Thermal diffusion of condenser water in a river.

Structures for condenser water discharge can be designed for the purpose of achieving a high degree of initial dilution or alternatively, to produce almost complete stratification – surface spreading of the warm water – in which case heat loss to the atmosphere is a major contribution to the reduction of excess temperature in the outfall area. An intermediate situation where both atmospheric heat exchange and mixing are important may be the most appropriate way of meeting water quality standards and reducing recirculation. A broad discussion of the mechanics of condenser water discharge in rivers has been given by Harleman (1969).

The data characterizing cooling water discharges may vary considerably from case to case. The following set of data are chosen as representative mean values:

Excess temperature of the discharged cooling water	$\Delta T = 10^{o}C$
The corresponding relative density difference	$\frac{\Delta\rho}{\rho} \approx 2.10^{-3}$
Rate of condenser water flow per unit diffuser length	$q = 0.3\ m^2/s$
The corresponding discharge velocity	$u_j = 1\ m/s$
Ambient river velocity	$u_a = 0.2\ m/s$
Depth	$H = 5\ m$

Hence, the momentum flux $m = 0.3\ m^2/s$ and the buoyancy flux $b = 6 \cdot 10^{-3}\ m^3/s^3$, and we have as governing parameters for these prototype conditions:

$k = 5$

$F = 1.3$ (F-values may vary considerably)

$V = 3$

θ varying

B. Marine disposal of sewage.

The density difference between the sea water and the sewage is usually about 25 kg/m^3, which gives a value of the relative density difference $\frac{\Delta\rho}{\rho} = 25 \cdot 10^{-3}$. Assume that the diffuser is designed for a discharge of 1 m^3/s sewage per 100 m length of the diffuser and that there is sufficient head to jet the sewage out horizontally at a velocity of 2 m/s. The depth may be 30 m and the ocean current perpendicular to the outfall pipe may have a typical speed of say 0.05 m/s. This will give us the following set of variables:

$$q = 0.01 \ m^2/s$$

$$m = 0.02 \ m^3/s^2$$

$$b = 2.5 \cdot 10^{-3} \ m^3/s^3$$

$$u_a = 0.05 \ m/s$$

$$H = 30 \ m$$

$$\theta = 0$$

The dimensionless numbers to define the flow problem are then:

$$k = 40$$

$$F = 0.05$$

$$V = 150$$

$$\theta = 0$$

III-3 Scale Models

Physical models are frequently used to study waste disposal problems. Therefore it could be of interest to add to the result of the dimensional analysis some considerations for the proper scaling of this type of flow phenomenon.

The basic concept of dynamic similarity requires that two systems of geometric boundary similarity have similar flow patterns at corresponding instants of time. In free surface flow the Froude number F_R defined below must be equal in model and prototype:

$$F_R = \frac{u_a^2}{g H} \tag{22}$$

To reproduce the density effects properly, the densimetric Froude number F_D must be equal in model and prototype:

$$F_D = \frac{u_a^2}{\frac{\Delta\rho}{\rho} g H} \tag{23}$$

If dynamic free surface effects must be modelled as well as buoyancy effects, the chosen relative density difference $\Delta\rho/\rho$ must remain unscaled. However, in diffusion models, similarity based on F_D only (the buoyancy effect) is usually sufficient and $\Delta\rho/\rho$ may be increased in the model to increase the model velocities.

The non-linearity of the equation of state

$$\rho = f \text{ (salinity, temperature)} \tag{24}$$

usually has to be considered when the reference values of salinity or temperature are selected in the model. Furthermore, dynamic similarity requires the individual jets of the outfall structure to be reproduced by the same jet Froude number F_j, previously defined, as in the prototype.

The effect of gravity is fairly easy to model, whereas it may be impossible to reproduce properly the viscous effects. In the model the Reynolds number, R_e, must be large enough to ensure turbulent flow conditions. Interfacial resistance generally depends on the Reynolds number, which may cause some scale effects in the model.

Thermal models require special considerations. A vertically distorted model may be necessary to simulate the heat exchange with the environment over a large area. But to reproduce the flow field in the immediate proximity of the diffuser, neither viscous effects nor heat dissipation should cause any serious scaling problems; see for instance Ackers (1969).

CHAPTER IV

A BUOYANT SLOT JET INTO STAGNANT ENVIRONMENT

IV-1 Theory

A theoretical solution for the case of a horizontal, buoyant slot jet in stagnant, homogeneous water has been presented by Abraham (1963). Abraham's solution follows the integral approach assuming that the lateral velocity and buoyancy profiles are approximately Gaussian. The theory is based on empirical functions for the spread of mass and momentum where the rate of spread is introduced as a function of the local angle of inclination of the jet trajectory. The following equations have to be solved:

two momentum flux equations

geometric relations for the jet trajectory

empirical spread relations for momentum and mass

Abraham makes the usual Boussinesq approximation, that is, that density differences can be ignored in all terms except the gravity term, and presents a numerical solution to his system of equations.

Fan and Brooks (1969) have presented a variety of numerical solutions to jet diffusion problems also, including the two-dimensional buoyant jet in uniform and linearly stratified environment. The angle of injection is left as a variable in these calculations. The theory is based on the principle of entrainment, first proposed by Morton, Taylor, and Turner (1956) which Fan and Brooks advocate as being more

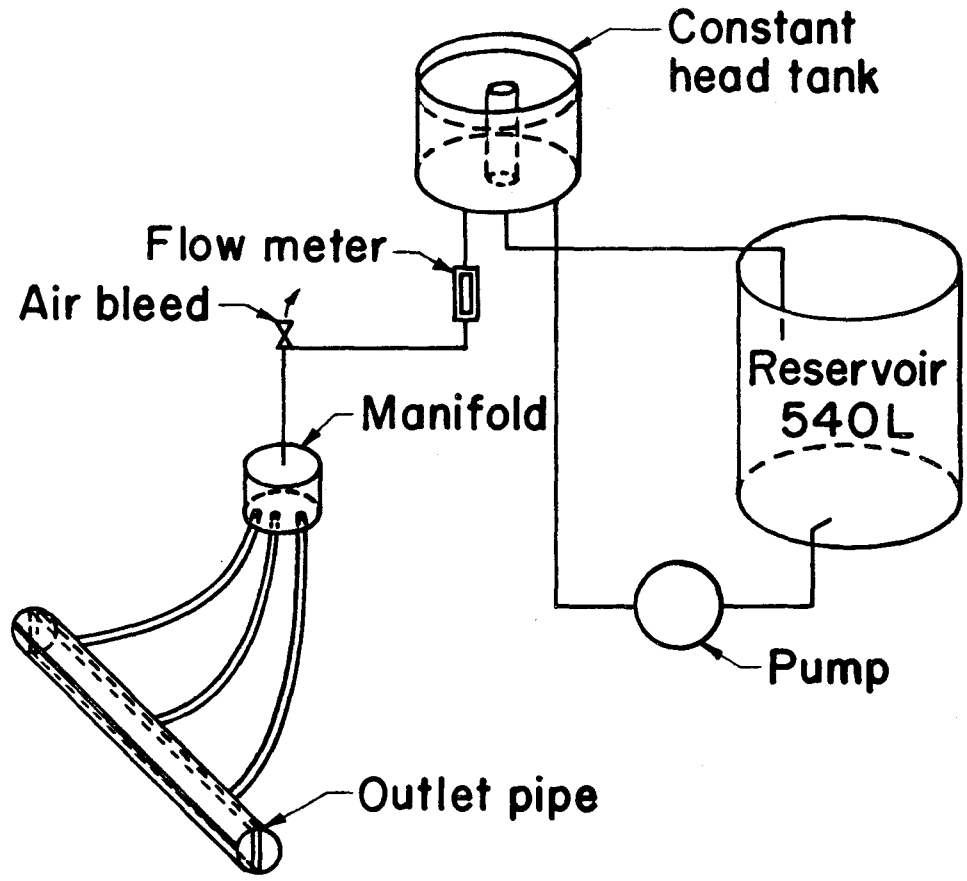

Fig. 3 Laboratory set-up for experiments with buoyant slot jets.

simple and more logical from a physical point of view. The concept of entrainment provides an equation for the conservation of the volume flux which actually was by-passed by Abraham. Hence, the following equations have to be solved

conservation of volume flux

two momentum flux equations

geometric relations for the jet trajectory

The two theories give practically the same result (Fan and Brooks (1966)).

IV-2 Laboratory Study.

Experiments were conducted in a 2-foot wide flume to determine the trajectories of the jet as well as the centerline dilution of the discharged effluent.* Figs. 3 and 4 show a sketch of the experimental set-up. A slot detail is given in Fig. 4. The slot width was 1/16 inch and the wall thickness of the outlet pipe 1/8 inch. With this aspect ratio of the slot, contraction of the jet could be neglected. Hence, the initial jet diameter equals the slot width. The outlet arrangement was found to produce a uniform efflux from the slot. Salt solutions were used to model the variation in density. Temperature differences were less than 2° C for all the test runs. Hence, the density variations induced by temperature fluctuations could be neglected. The experiments were performed by jetting heavier salt solutions into fresh water. Because similarity is achieved according to Froude's law (F_j is significant not F_R), it makes no difference whether the apparent gravity acts up or down. This technique has been employed previously in laboratory studies on jet diffusion, see Fan (1967) and Cederwall (1968).

---

* The build-up of a surface field of jet effluent mixture in a stagnant environment may be the design condition in a real case considering water quality requirements. This hydraulic problem has not been studied.

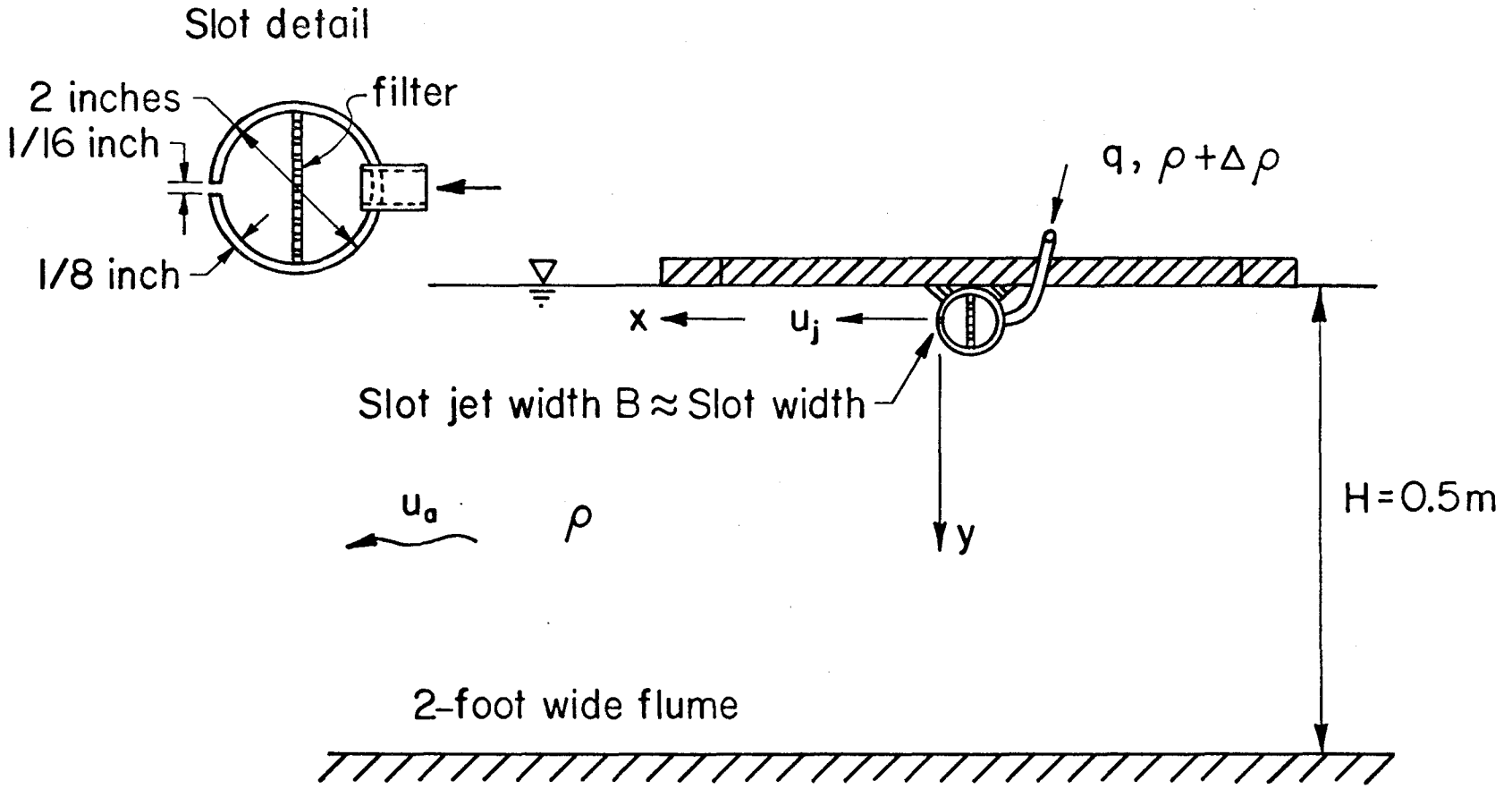

Fig. 4 Outlet arrangements for experiments with a buoyant slot jet.

Two methods were used for determining centerline concentration and the curvature of the jet: in-situ measurements with a conductivity probe or sampling with a simple sucking device. The conductivity probe was developed at the W. M. Keck Laboratory, California Institute of Technology; see Fig. 5. A detailed information sheet on the probe design is given by Okoye (1970). The probe was mounted on a tiltable point gage, fixed to a carriage on top of the flume. For calibration of the probe, standard solutions were used prepared from dry salt dissolved in distilled water. Hence, the background salinity of the flume water had to be accounted for when evaluating the dilution. A single channel Sanborn recorder with an 1100 AS Carrier Pre-Amplifier was used. The bridge circuit for the conductivity measurements is described by Koh (1964). In addition, photos were taken to study the gross behavior of the jet. Since the experimental technique was essentially the same as used by the references cited above, no detailed description of the procedure will be given in this report.

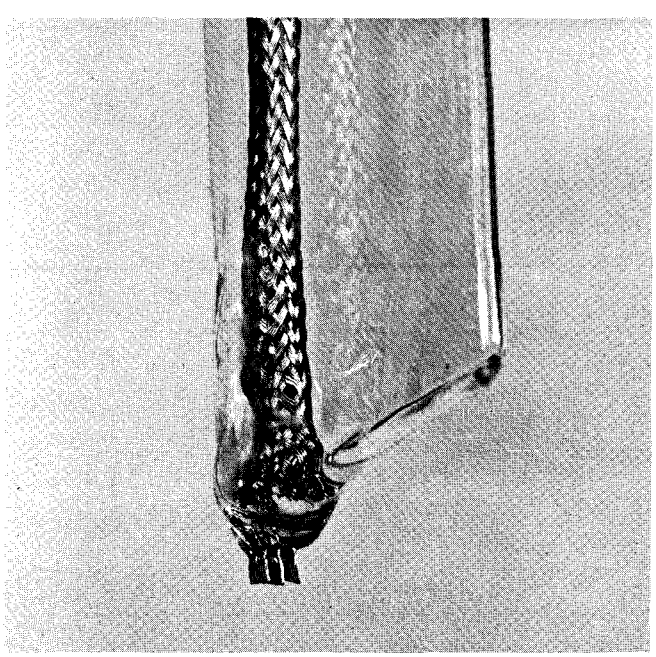

Fig. 5 The conductivity probe. The three electrodes are 1/8-inch square each and spaced 1/16-inch apart. The two outside plates are electrical ground.

Table 1. Experiments with horizontal buoyant slot jets in stagnant, uniform environment. The initial slot jet width B=1.57 • 10^{-3} m.

RUN	F_j	Position of jet axis at sampling section y cm	x cm	Centerline dilution S_m
1	17.2	4.9	10.4	5.2 *
2	18.9	13.8	18.0	9.2 *
3	16.1	13.7	16.0	9.8 *
4	25.2	12.0	22.6	8.2 *
5	15.2	27.0	16.2	15.1
6	20.7	19.2	19.8	13.8
7	17.2	17.6	18.5	11.5
8	16.8	33.5	20.5	19.0
9	15.0	33.5	18.5	19.6
10	15.2	28.8	16.7	17.8
11	19.6	24.0	21.4	13.2
12	14.8	15.7	14.3	12.9
13	16.0	9.0	11.9	7.8
14	19.6	9.2	15.3	8.6
15	13.6	6.6	8.6	7.4

* Determined from in-situ measurements with a conductivity probe; the other data are from sampling.

The experimental variables ranged as follows:

$$B = 1.57 \cdot 10^{-3}\ m$$

$$H = 0.50\ m$$

$$\frac{\Delta\rho}{\rho}: \text{ varied from } 4 \cdot 10^{-3} \text{ to } 17 \cdot 10^{-3}$$

$$u_j: \text{ varied from } 0.2 \text{ to } 1.0\ m/s$$

$$\theta = 0$$

The jet Reynolds number, defined as

$$R_{ej} = \frac{2 u_j B}{\nu} \tag{25}$$

where ν is the kinematic viscosity, ranged from about 600 to 3000. The jet flow was always turbulent. The results of the experimental runs are listed in Table 1.

Fig. 6 shows experimental data from measurements in-situ with the conductivity probe. The centerline dilution S_m is defined by

$$S_m = \frac{c_o - c_b}{c_m - c_b} \tag{26}$$

where c_o and c_b are the concentrations of the jet effluent and the background concentration of the ambient water respectively. c_m is then the estimated centerline concentration to give the best fit to a Gaussian distribution of the lateral concentration profile. c is a local concentration measured within the jet. In Fig. 6, $\frac{c - c_b}{c_m - c_b}$ was plotted against $(r/\lambda b)^2$ on a semi-log graph where r is the lateral coordinate, b the nominal half-width of the jet according to theory of Fan and Brooks (1969), and λ a spreading ratio between mass and momentum given a value 0.89 as suggested by these authors. r = 0 was established by measuring on both sides of the plume axis. It is obvious from the graph of Fig. 6 that a Gaussian distribution fits the data, and that observed and predicted rate of jet expansion are in good agreement.

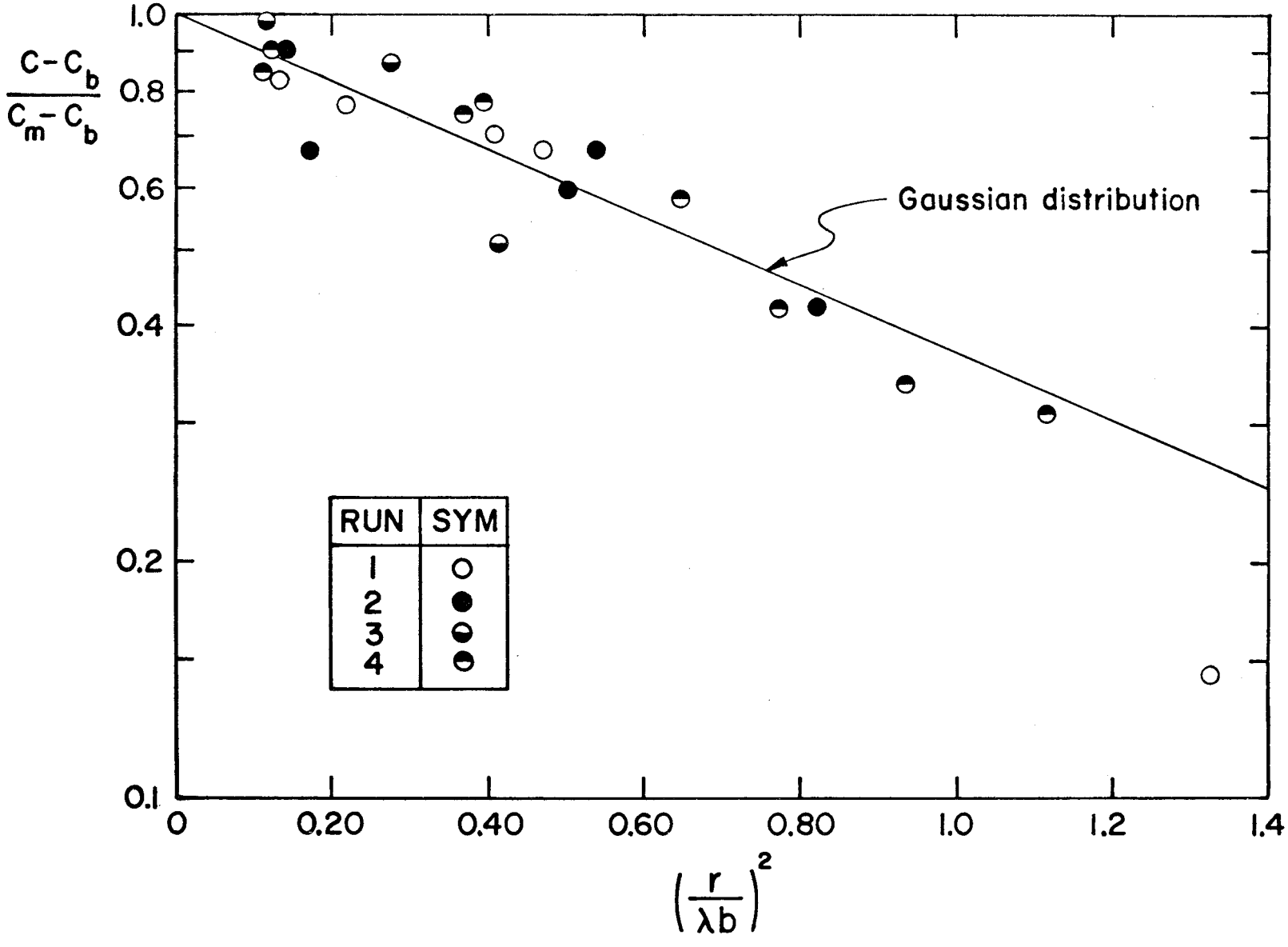

Fig. 6 Observed lateral distributions of concentration for horizontal, buoyant, slot jet in stagnant environment.

Let x and y be the horizontal and vertical coordinates respectively. When plotting the jet trajectory $\frac{x}{B}$, $\frac{y}{B}$ it follows from dimensional arguments that F_j is a single free parameter when the effect of viscosity can be neglected. Analyzing the set of equations that Abraham proposes for solving the problem of the horizontal slot jet, we find that the following relations hold for the jet curvature:

$$\frac{y}{B} \cdot F_j^{-4/3} = f_1(\beta) \tag{27}$$

$$\frac{x}{B} \cdot F_j^{-4/3} = f_2(\beta) \tag{28}$$

where β is the local angle of inclination of the jet trajectory. The effect of the zone of flow establishment has then been neglected requiring that the point on the trajectory is not too close to the source. Hence, using Abraham's approach that specifies the rate of growth of the jet as a function of β, the theoretical jet paths collapse when plotted on a graph of $\frac{y}{B}F_j^{-4/3}$ vs. $\frac{x}{B}F_j^{-4/3}$. It can also be shown that Abraham's theory leads to a similar result for the three-dimensional buoyant jet where $\frac{y}{D}F_j^{-1}$ is a unique function of $\frac{x}{D}F_j^{-1}$. (D is then the jet diameter.)

Fig. 7 is a graphical representation of the theoretical jet curvatures with the dimensionless coordinates chosen as $\frac{y}{B}F_j^{-4/3}$ and $\frac{x}{B}F_j^{-4/3}$. The jet trajectories determined by the theory suggested by Fan and Brooks do not collapse; however, as shown by the graph, the curves for $F_j = 8$ and $F_j = 32$ are fairly close. A constant α-value of 0.16 and $\lambda = 0.89$ were used to calculate these curves, which choice assumes the buoyancy effect on the entrainment to be predominant (see Fan and Brooks (1969)).

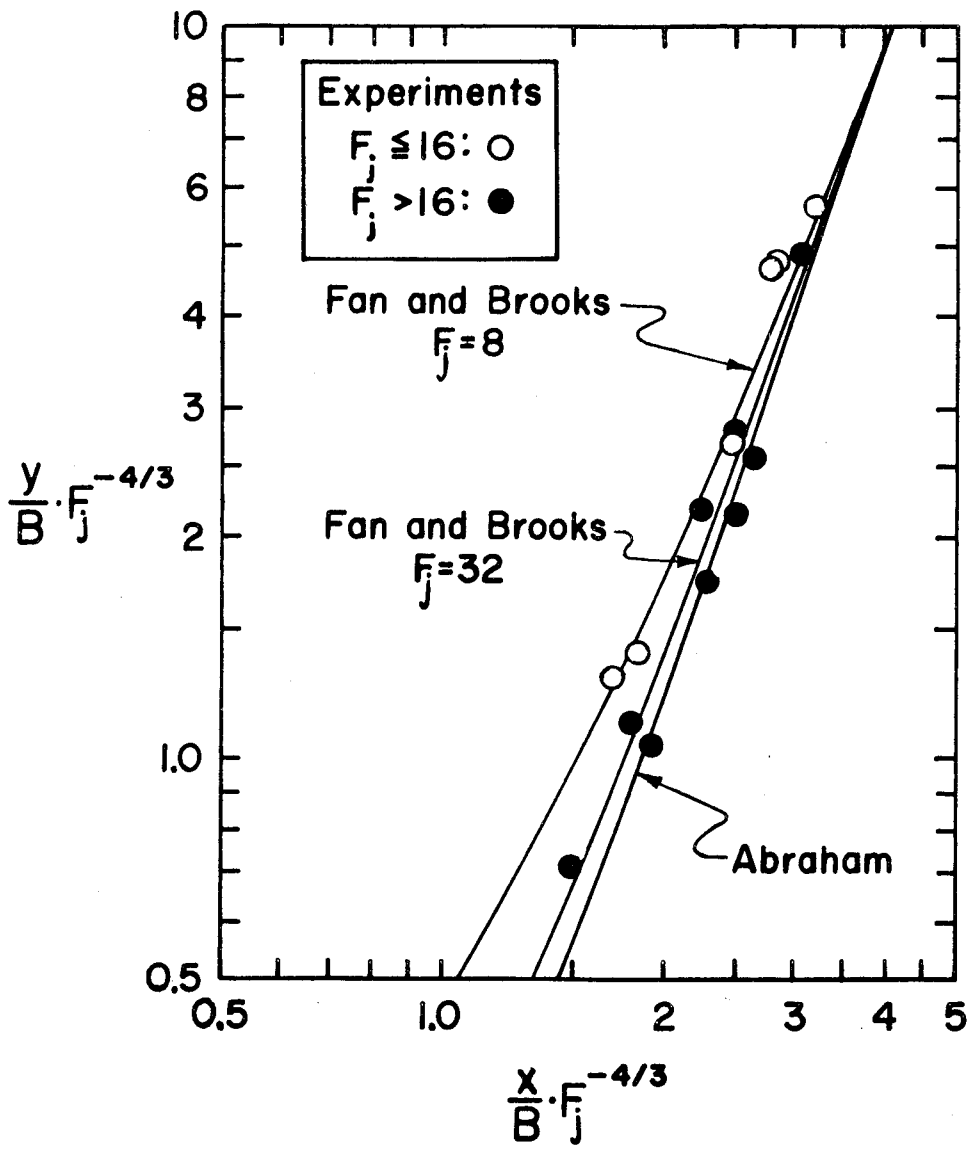

Fig. 7 Graphical representation of the theoretical jet trajectory for a horizontal, buoyant slot jet in stagnant environment and comparison with experimental data. The curves of Fan and Brooks (1969) are based on $\alpha = 0.16$ and $\lambda = 0.89$.

The parameters chosen for the graphical representation of the jet trajectory make comparison between theory and experiment very convenient. The experimental data seem to fit the theory of Fan and Brooks better than Abraham's – especially for $F_j < 16$.

It would be convenient to have a graphical representation of the centerline dilution similar to the jet curvature, not only for design purposes, but also for comparing theoretical and observed dilution data. If we again look at Abraham's solution technique, we find that the following relation can be deduced from the basic equations

$$S_m \left(\frac{y}{B}\right)^{-\frac{1}{2}} = f_3(\beta) \tag{29}$$

Hence, Abraham's approach gives $S_m \left(\frac{y}{B}\right)^{-\frac{1}{2}}$ as a unique function of, for instance, $\left(\frac{y}{B}\right)^{\frac{1}{2}} F_j^{-\frac{2}{3}}$. (Similarly for the three-dimensional jet, $S_m \left(\frac{y}{D}\right)^{-1}$ is a function of $\frac{y}{D} F_j^{-1}$). This grouping of the parameters takes the case studied by Rouse, Yih and Humphreys (1952) who gave the centerline dilution for a two-dimensional plume as: *

$$S_m = 0.39 \left(\frac{y}{B}\right) F_j^{-\frac{2}{3}} \qquad F_j \text{ small} \tag{30}$$

It is interesting to note that the theoretical solution of Fan and Brooks almost collapses into one curve when plotted in a graph of $S_m \left(\frac{y}{B}\right)^{-\frac{1}{2}}$ vs. $\left(\frac{y}{B}\right)^{\frac{1}{2}} F_j^{-\frac{2}{3}}$ (see Fig. 8). For F_j ranging from 8 to 32 the deviation between the curves is negligible. The position of the curve of Fan and Brooks for

---

* In terms of dilution their result was actually $S_m = \frac{g}{2.6} \frac{\Delta\rho}{\rho} b^{-\frac{2}{3}} y$. We arrive at Eq. (30) by defining b according to Eq. (3). Hence, Eq. (30) is a true plume solution despite the fact that F_j appears as flow parameter.

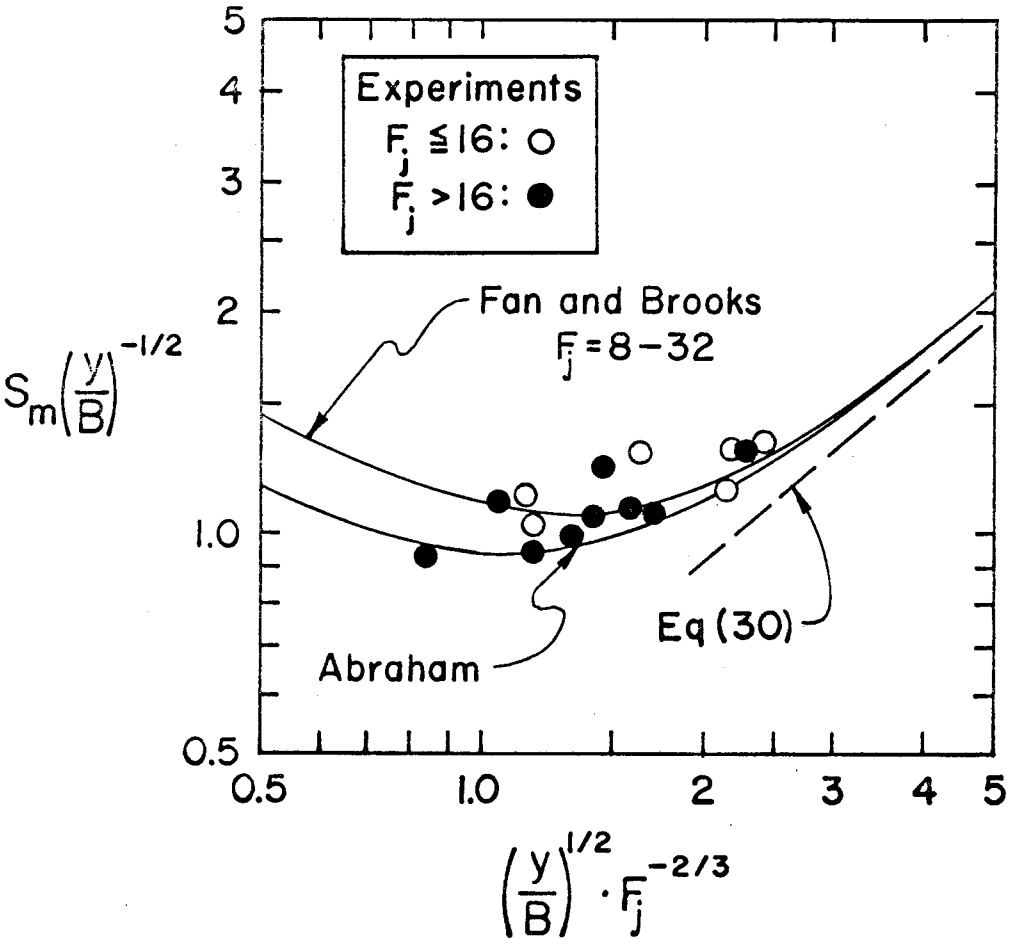

Fig. 8 Graphical representation of the theoretical centerline dilution for a horizontal, buoyant slot jet in stagnant environment and comparison with experimental data. The theoretical relation of Fan and Brooks (1969) is based on $\alpha = 0.16$ and $\lambda = 0.89$.

$F_j = 8 - 32$ depends on the choice of value of the coefficients α and λ. By varying λ, keeping α constant, the curve moves horizontally whereas a change in α, with λ constant, moves points on the curve along a straight line with the slope -1, if a log-log paper is used. For $\alpha = 0.16$ and $\lambda = 0.89$, the solution of Fan and Brooks coincides with that of Abraham in the range of $\left(\frac{y}{B}\right)^{\frac{1}{2}} \cdot F_j^{-\frac{2}{3}}$ where the buoyancy effect on the mixing is predominant but the curves differ significantly in the range of $\left(\frac{y}{B}\right)^{\frac{1}{2}} F_j^{-\frac{2}{3}}$ where initial flux of momentum predominates, i. e. close to the source. To get the curves to collapse in this range of $\left(\frac{y}{B}\right)^{\frac{1}{2}} F_j^{-\frac{2}{3}}$ the value of α has to be reduced to about 60%, that is from 0.16 to 0.095. The latter value is rather close to the α value that has been found characterizing a two-dimensional momentum jet, that is $\alpha = 0.069$.

The experimental data are in reasonable agreement with the theories.

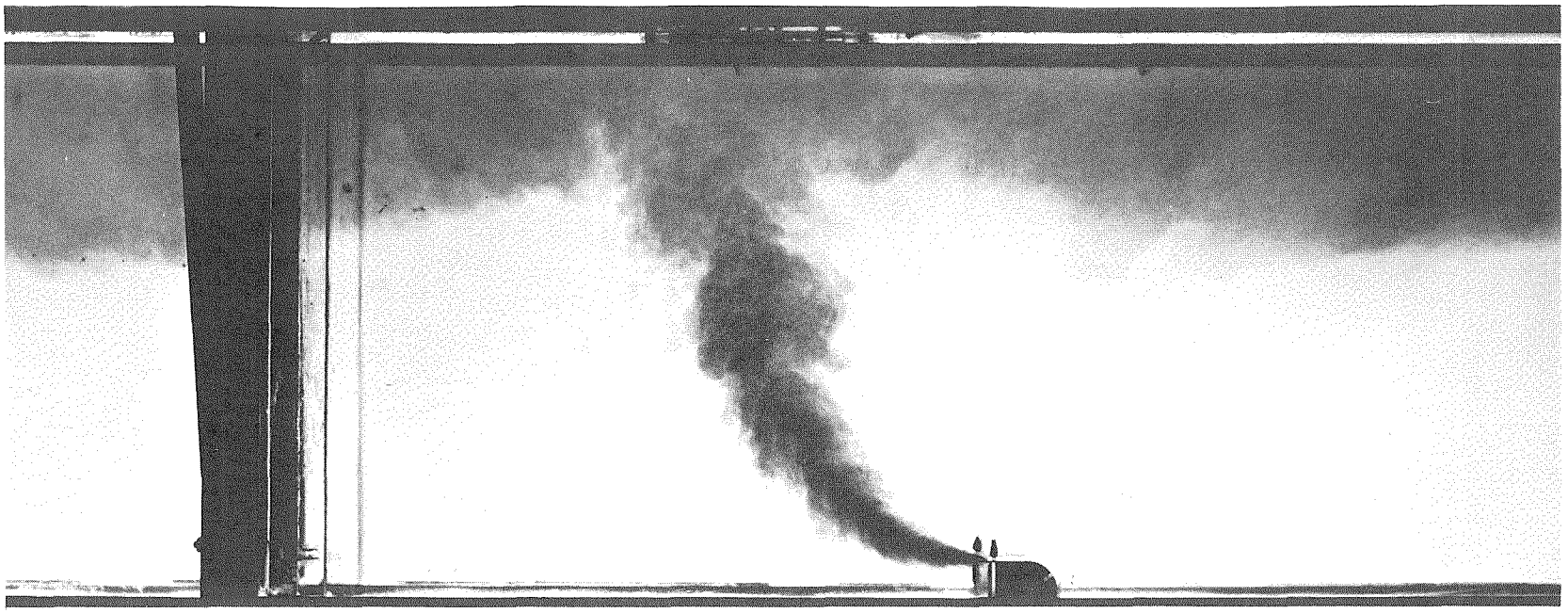

10225

Fig. 9 A horizontal, buoyant, slot jet in stagnant, ambient fluid. $u_a \equiv 0$, $F_j = 10.2$.

CHAPTER V

A BUOYANT SLOT JET INTO A FLOWING ENVIRONMENT

A natural body of water such as the ocean is always in motion. Ocean currents not only affect the transportation and spreading of the established sewage field following the disposal of waste water, but also change the jet mixing characteristics. Even if the current speed is very small in relation to the jet velocity, the current effect can still be significant. Similarly, in rivers and estuaries there are problems of initial mixing not sufficiently studied.

In this chapter we will discuss the gross behavior of a buoyant slot jet in a confined, uniformly flowing environment. This represents theoretically a very complex problem since there are three vector quantities involved; namely, the initial flux of momentum, the ambient flow and gravity. We will find that the typical jet or plume flow pattern does not exist for a wide range of the governing parameters. Hence, an extension of the integration technique used successfully for solving many jet and plume problems in a stagnant environment has no general application to the present flow phenomenon. This study will be mainly empirical, the primary objective being to find dimensionless criteria for the basic flow regimes.

V-1 Experimental Procedure

Experiments were conducted in the 2-foot wide flume previously used for the tests with a stagnant ambient fluid, Fig. 10. Most of the runs, however, were made in a 6-inch wide flume well suited for photographic

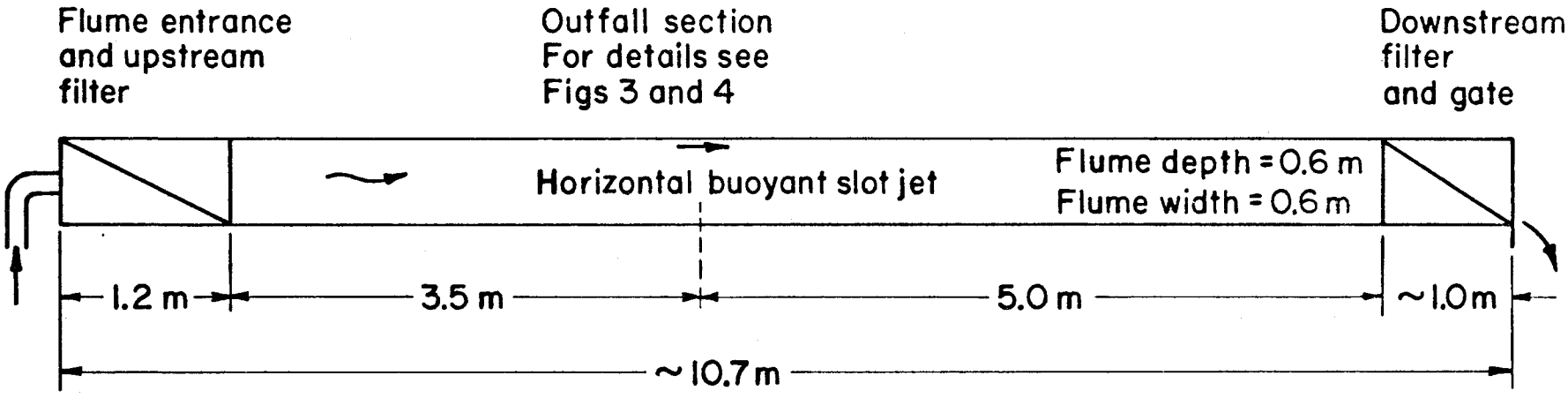

Fig. 10. The 2-foot wide flume in section used for experiments with a horizontal, buoyant slot jet.

recording of the flow pattern, Fig. 11. The maximum flow depth of both of these flumes is about 0.5m. The flume velocities varied from 0.01 m/s to about 0.06 m/s. By injecting vertical streaks of dye into the flume the upstream and downstream filters were adjusted to provide a uniform flow field and the velocity was determined.

Apart from having flowing water in the flume, the experimental procedure was very much the same as described in Chapter IV. Heavier jet effluent was injected into the ambient flow at the surface. As boundary layer effects were small, this case is equivalent to injecting lighter fluid at the bottom of the flume. The photos of Figs. 15 to 18 have been turned upside down to illustrate this latter flow situation in agreement with the basic assumptions as given by the definition sketch of Fig. 1. The smaller flume had an injection device which allowed the slot width and the angle of injection to vary (see Fig. 11). The background level of salinity and dye was kept low by frequently changing the reservoir waters of the flumes.

V-2 Predicted Flow Regimes

We may define two different flow regimes depending on whether or not there occurs upstream intrusion of the mixture of jet effluent and ambient fluid. This phenomenon is essentially the same as we find in partly mixed estuaries: saltwater intrusion caused by the density difference between fresh and saline water. In the present case, however, we may have a surface wedge of diluted "waste water" that penetrates upstream of the outfall since we have assumed that the discharged fluid was lighter than the ambient fluid.

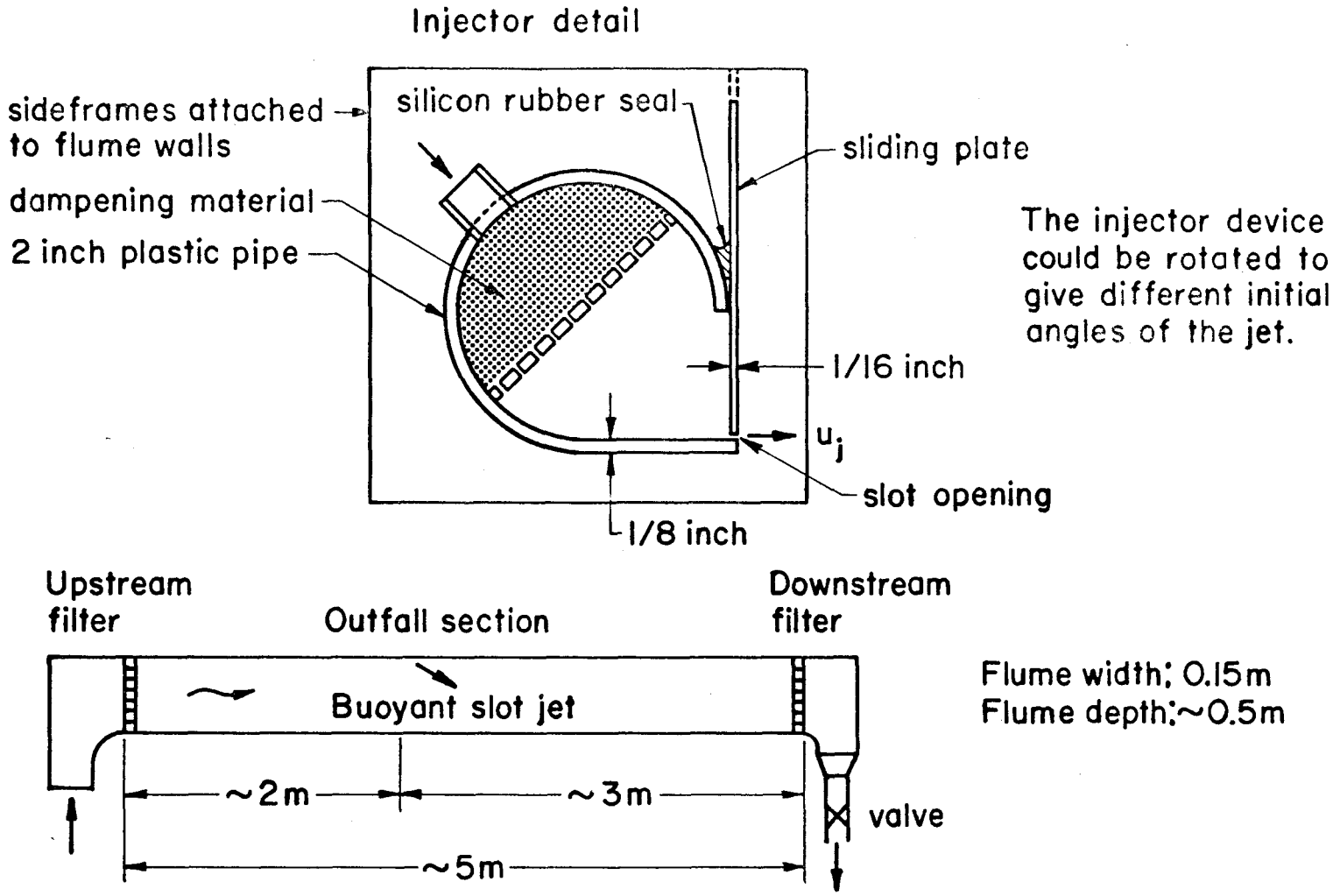

Fig. 11 Section of the 6-inch wide flume with slot detail used for experiments with a buoyant slot jet.

The mechanism of intrusion of a surface wedge is described by the stratified flow system shown in Fig. 12. Assume steady flow and homogeneous, immiscible layers differing by $\Delta\rho'$ in density. Q_1 and Q_2 are the flow rates of the two layers per unit width. If the bottom is horizontal and we neglect vertical accelerations, the equations of motion may be written as

$$-\rho \frac{d}{dx}\left(\frac{Q_1^2}{H_1}\right) = -\rho g H_1 \frac{dH}{dx} + \tau_i \tag{31}$$

$$(\rho+\Delta\rho') \frac{d}{dx}\left(\frac{Q_2^2}{H_2}\right) = -\rho g H_2 \frac{dH}{dx} - \Delta\rho' g H_2 \frac{dH_2}{dx} - (\tau_i+\tau_b) \tag{32}$$

$$H = H_1 + H_2 \tag{33}$$

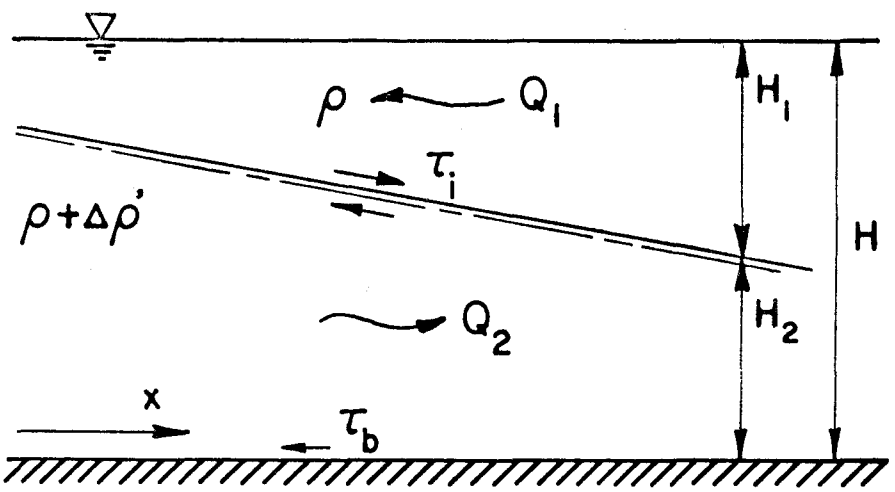

Fig. 12 Two-layer stratified flow system.

To describe the arrested surface wedge situation (see Fig. 13) assume $Q_1 \equiv 0$. Using a Boussinesq assumption Eqs. (31) and (32) reduce to

$$\left(\frac{Q_2^2}{H_2^2} - \frac{\Delta\rho'}{\rho} g H_2\right) \frac{dH_2}{dx} = \frac{1}{\rho}\left(\tau_i \frac{H}{H_1} + \tau_b\right) \tag{34}$$

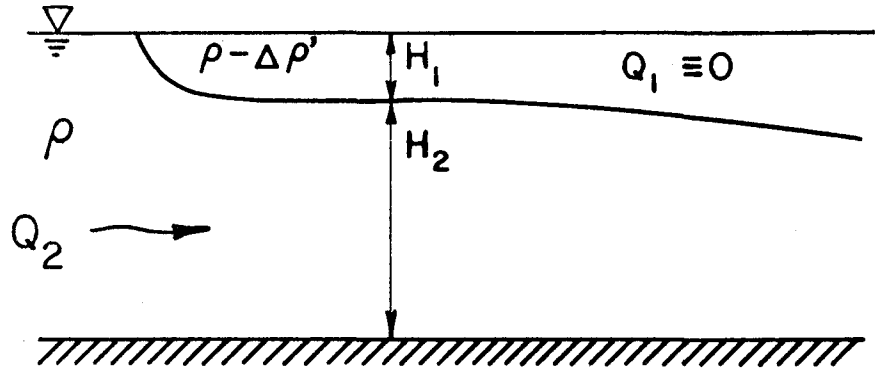

Fig. 13 An arrested surface wedge.

The following definitions are made

$$F_D = \frac{Q_2^2}{\frac{\Delta\rho'}{\rho} gH^3} = \frac{u_a^2}{\frac{\Delta\rho'}{\rho} gH}$$

$$\tau_i = \rho A^2 \left[\frac{Q_2}{H_2}\right]^2$$

$$\tau_b = \rho B^2 \left[\frac{Q_2}{H_2}\right]^2 \qquad (35)$$

$$\eta = \frac{H_2}{H}$$

$$\xi = \frac{x}{H}$$

where A and B are constants relating the shear stresses to the mean velocity.

Eq. (34) may now be written

$$\frac{d\eta}{d\xi} = \frac{A^2 + B^2 (1 - \eta)}{(1 - F_D^{-1} \eta^3)(1 - \eta)} \qquad (36)$$

which is the normalized differential equation for the arrested surface wedge ($Q_1 \equiv 0$), and is very similar to the corresponding relation for an arrested bottom wedge.

For an arrested surface wedge $\frac{d\eta}{d\xi} < 0$. As the factor $(1-\eta)$ in the denominator of Eq. (36) is small but positive then $(1 - F_D^{-1} \eta^3)$ must be negative or,

$$F_D < \eta^3 \ . \tag{37}$$

Since $\eta = 1$ upstream of the wedge, a necessary condition for the wedge to form is $F_D < 1$; otherwise negative values of $\frac{d\eta}{d\xi}$ are impossible. A dimensionless critical depth η_c may be defined as: $\eta_c = \sqrt[3]{F_D} = H_c/H$ and ,

$$\eta_c < \eta < 1 \tag{38}$$

for an arrested wedge.

A densimetric Froude number characterizing the flow of the lower layer is written (see Fig. 13):

$$\frac{Q_2^2}{\frac{\Delta\rho'}{\rho} g H_2^3} = \frac{Q_2^2}{H^3 \frac{\Delta\rho'}{\rho} g} \left(\frac{H}{H_2}\right)^3 = F_D \eta^{-3} = \left(\frac{\eta_c}{\eta}\right)^3 \tag{39}$$

and is always ≤ 1. For occurrence of critical flow, there must be a control such as an overfall or sill (as for ordinary open channel flow).

A critical condition was first formulated by Stommel and Farmer (1953) for the surface flow at the transition to the ocean in case of a salt-water wedge penetrating upstream in a river (Fig. 14b). For a surface wedge, a critical flow situation may be established, for instance, above an outfall pipe lying on the river bottom causing the flow section to be locally reduced. Hence, referring to Fig. 14a we have $Q_2^2 / \left[(H_2 - \Delta Z)^3 g \frac{\Delta\rho'}{\rho}\right] = 1$.

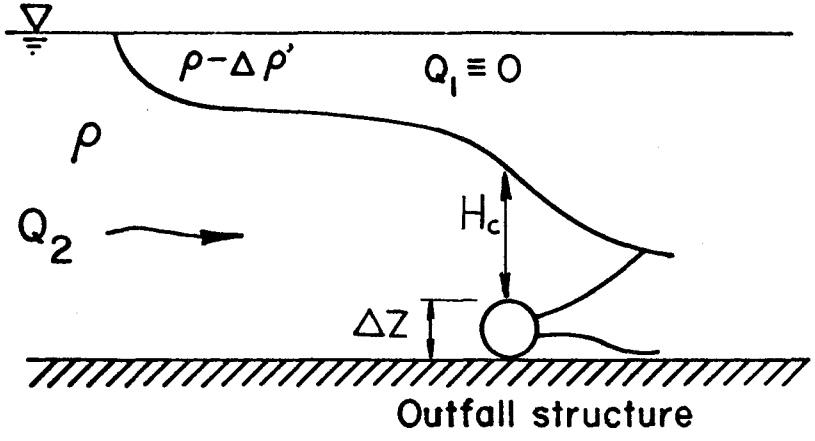

Fig. 14(a) Critical flow of the lower layer established above an outfall structure.

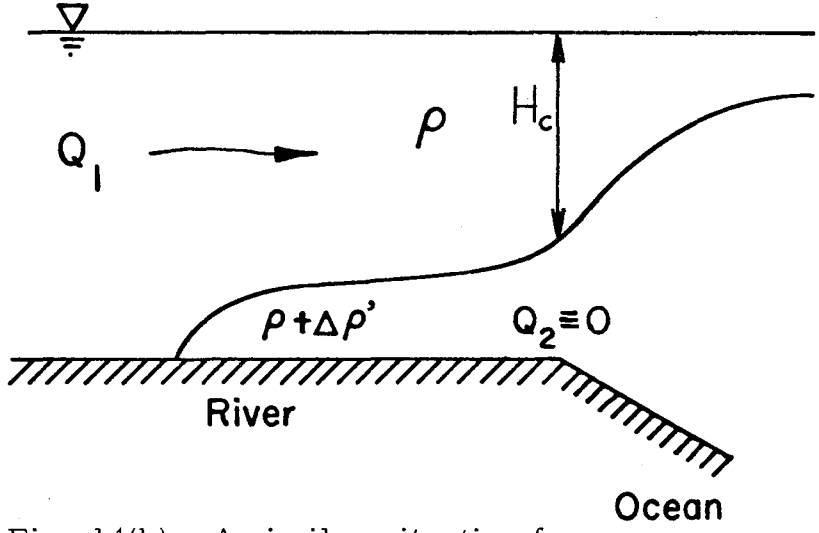

Fig. 14(b) A similar situation for a salt water wedge penetrating upstream in a river. The flow of the surface layer is critical at the transition to the ocean.

In order to completely expel the wedge in a section where the flow is critical, $\eta_c \to 1$, and consequently, as a criterion for no upstream intrusion of the surface wedge, F_D must be equal to or greater than one.

In case of a buoyant slot jet discharged at the bottom of the flume, the density difference must be reduced to account for the effect of mixing. Assuming complete mixing, the initial density difference of the efflux, $\Delta\rho/\rho$, should be divided by the volume flux ratio V in order to get $\Delta\rho'/\rho$ for the two-layer system; thus

$$F_D = \frac{Q_2^2}{\left(\frac{\Delta\rho g}{\rho V}\right)H^3} = \frac{u_a^3}{b} = F \tag{40}$$

Hence, assuming complete mixing between jet effluent and ambient flow, the criterion for no upstream intrusion states that $F \geq 1$. However, the relative density deficiency of the jet effluent mixture reaching the surface layer may exceed $\Delta\rho/(\rho V)$ due to poor mixing. In such a situation the criterion for no upstream intrusion has to be reformulated as

$$\frac{Q_2^2}{\left(\frac{\Delta\rho g}{\rho S}\right)H^3} = F \cdot \frac{S}{V} \geq 1 \text{ or } F \geq \frac{V}{S} \tag{41}$$

where S is the actual dilution of the jet effluent in the surface region. $S \leq V$ and hence $F \geq \frac{V}{S} \geq 1$.

The discussion so far has been based on the one-dimensional analysis of the simple stratified flow system defined by Fig. 12. The complexity of the problem is well described by Benjamin (1968) in his paper on "Gravity Currents and Related Phenomena". Benjamin finds that the dynamical coupling between the two phases of the flow system is an essential factor. In case of great depth relative to the thickness

of the upper layer – the uncoupled situation – the velocity of the wedge may be estimated by assuming energy-conserving flow. The relative speed of the wedge is found to be critical or close to critical (the densimetric Froude number of the surface flow is unity or close to unity) which result is also confirmed by experiments, Abbot (1961). Hence, in case of complete mixing between jet effluent and oncoming flow the arrested surface wedge is characterized by

$$u_a \approx \left[\left(\frac{\Delta\rho}{\rho} \cdot \frac{1}{V}\right) gh\right]^{\frac{1}{2}} \qquad (42)$$

$$\frac{h}{H} \text{ small}$$

where h is some typical thickness of the upper layer close to the tip of the wedge. From Eq. (42) follows that

$$F = \frac{u_a^3}{b} \approx \frac{h}{H} < 1 \qquad (43)$$

describes an arrested surface wedge which is thin relative to the depth of the flow.

The one-dimensional analysis of the two-layer flow system provided us with the framework for classification of flow regimes. It emphasized the significance of the source Froude number F for describing upstream intrusion of jet effluent. However, there are other features of the present diffusion problem more related to the characteristics of the source which in this case has both initial flux of momentum and buoyancy. The general flow situation is surprisingly complex and any attempt to formulate dimensionless flow regime criteria must be based on experimental findings. Hence, let us first look at some results of the experimental investigation.

Fig. 15 shows a critical situation with respect to upstream intrusion of jet effluent observed in one of the test runs with horizontal, buoyant slot jets. In this study critical flow will be defined as the situation in which the formation of a surface wedge is incipient at a reference section. The reference section indicated in Fig. 15 is pushed downstream of the outfall about two flow depths due to the effect of initial flux of momemtum.

Similarly, Fig. 16 illustrates a subcritical flow situation. The wedge has penetrated a short distance upstream from the reference section and is arrested; that is, the velocity of propagation induced by the density deficit is balanced by the velocity of the ambient flow.

Another flow situation is illustrated by a vertical slot jet having a high rate of initial flux of momentum. The jet flow then hits the surface almost perpendicularly and an upstream wedge is due to the very effect of the deflection at the surface (see Fig. 17). On the other hand, if the rate of entrainment of horizontal momentum relative to the flux of vertical momentum is high, the jet is bent over and may be swept downstream when reaching the surface (see Fig. 18). In this particular case, the upstream intrusion of the jet effluent is hampered.

The over-all mixing between jet effluent and ambient flow downstream of the outfall is of special interest from an engineering point of view. The rate of dilution of the discharged fluid is, for instance, a measure of the rate of temperature reduction in the case of a thermal waste-water discharge.

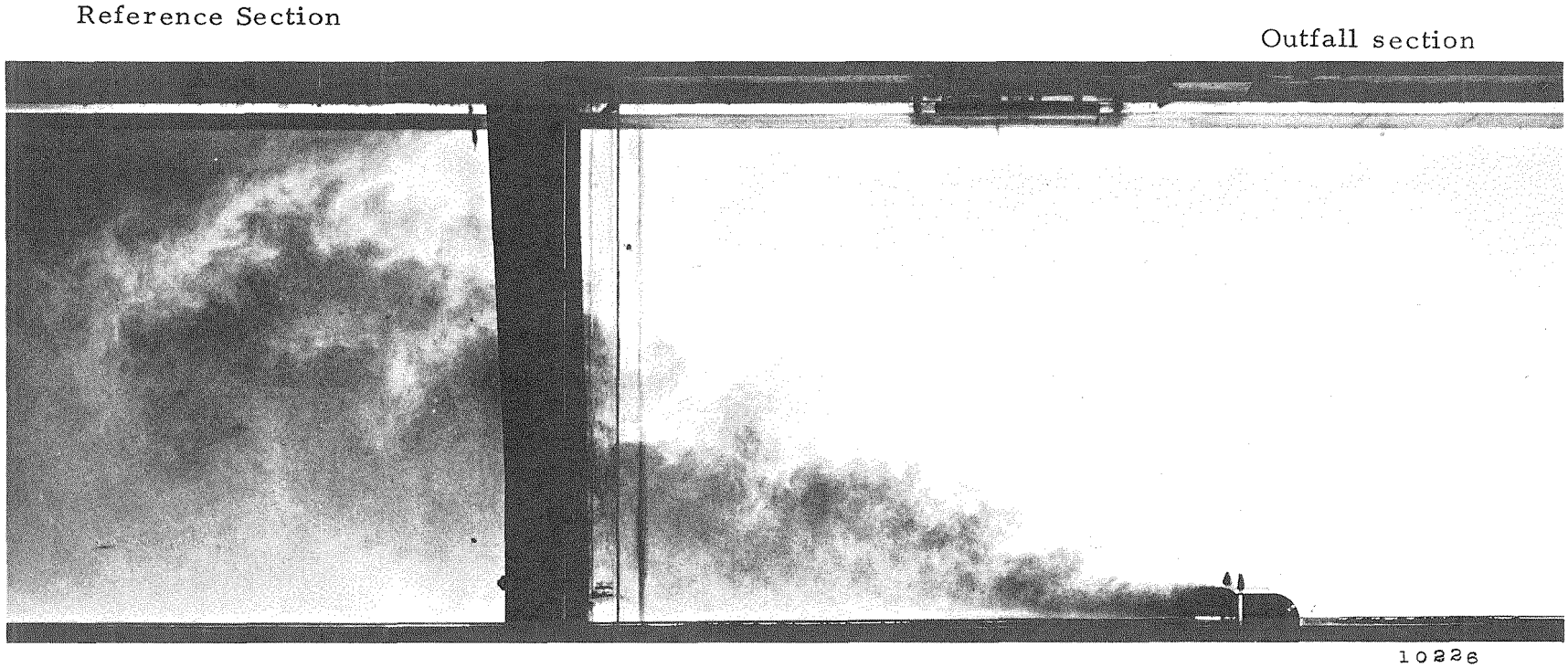

Fig. 15 A horizontal, buoyant, slot jet in a co-flowing stream. The surface wedge is completely expelled. F = 0.90; V = 50; and k = 8.

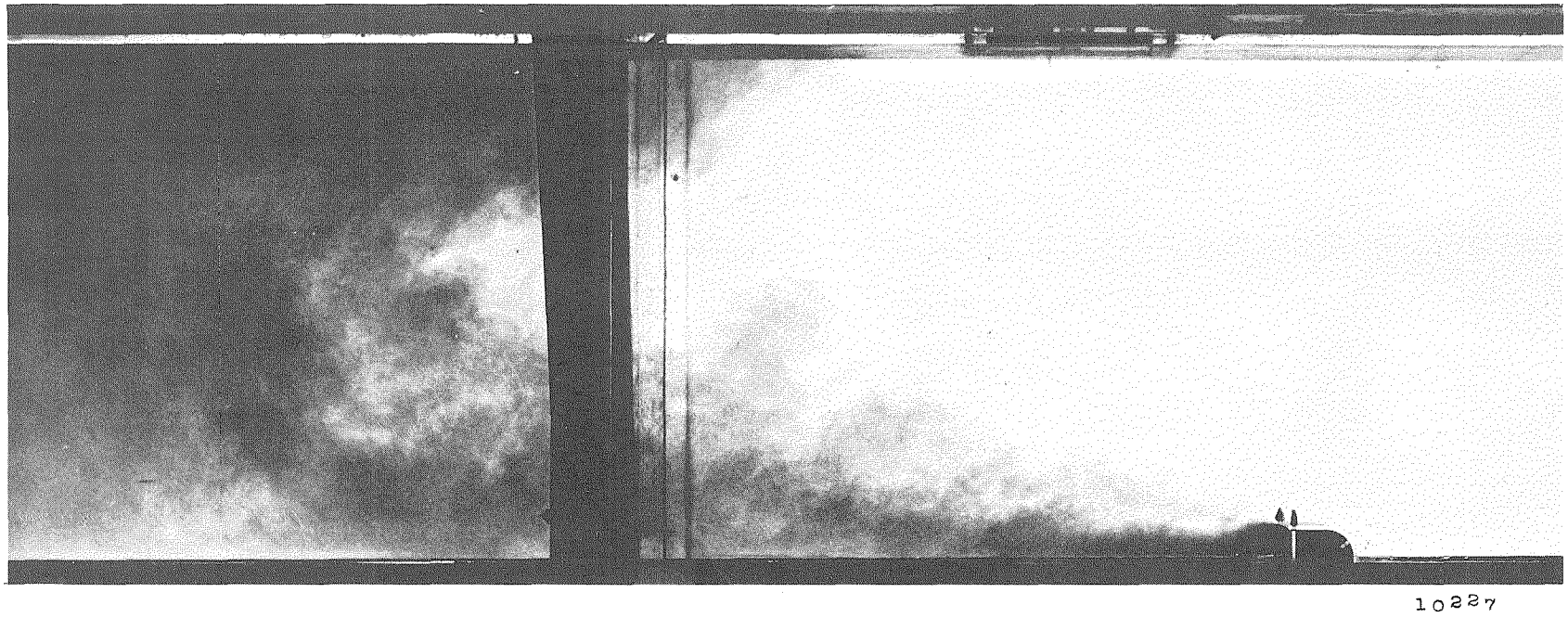

Fig. 16 A horizontal, buoyant, slot jet in a co-flowing stream. The surface wedge penetrates a certain distance upstream from the reference section. F=0.48; V=27; and k=15.

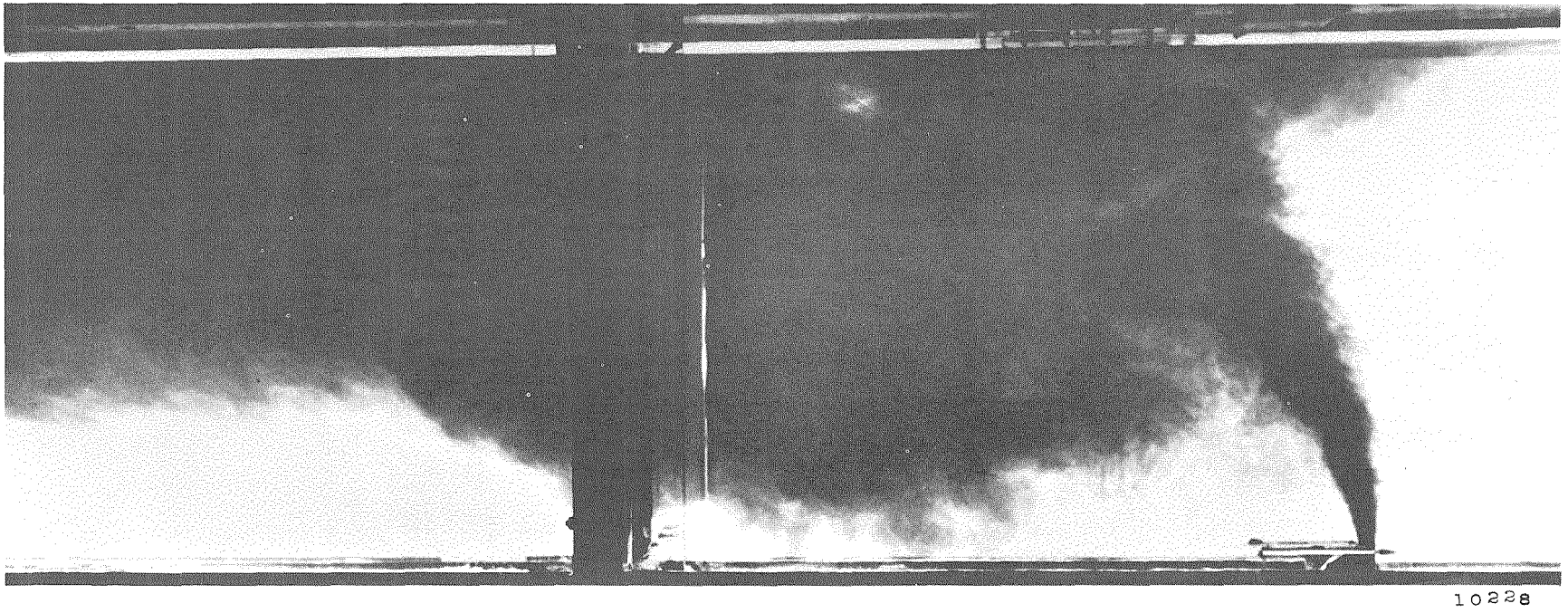

Fig. 17 A vertical, buoyant, slot jet in a cross stream. The wedge is due to the effect of deflection at the surface. Run 84. F=0.13; V=9; and k=41.

Depending on the downstream conditions, the "unpolluted" water volumes downstream of the blocking outfall jet may ultimately be recirculated by water mixed with jet effluent.

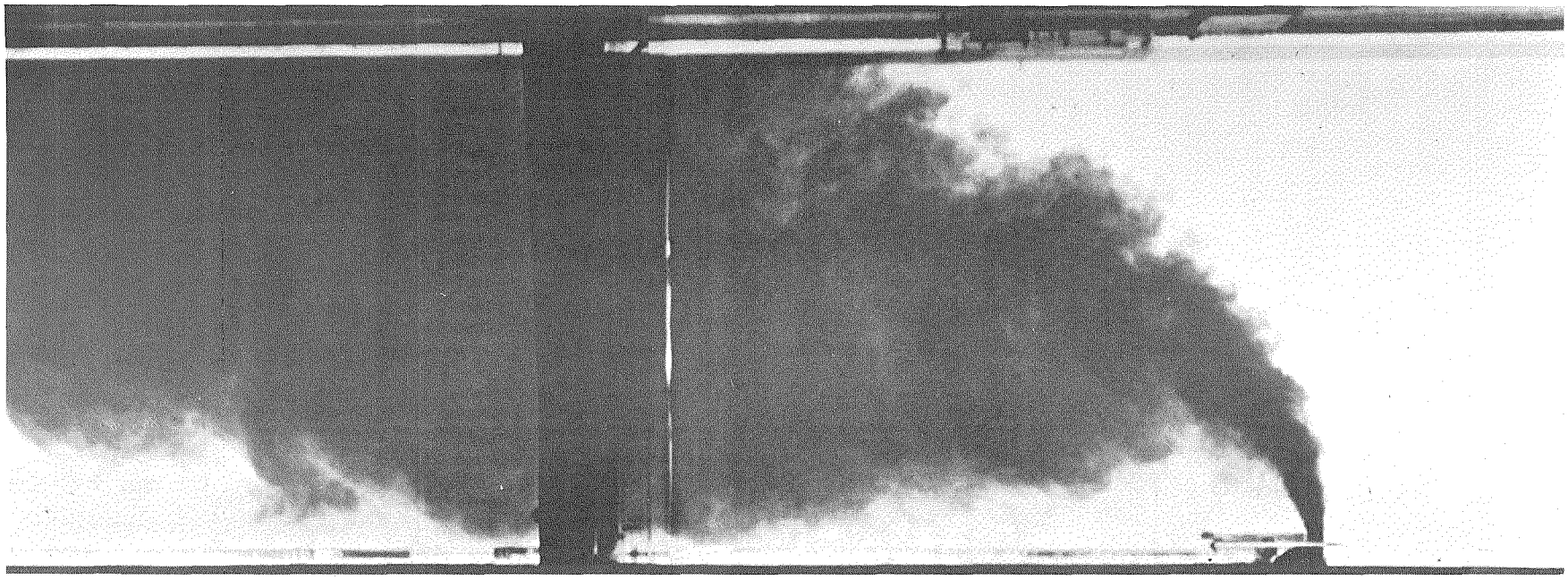

10229

Fig. 18 A vertical, buoyant, slot jet in a cross stream. The jet flow is swept downstream due to entrainment of horizontal momentum of ambient flow. Run 83. F=0.57; V=23; and k=17.

Depending on the downstream conditions, the "unpolluted" water volumes downstream of the blocking outfall jet may ultimately be recirculated by water mixed with jet effluent.

In a confined region the oncoming flow will always be completely entrained by the flow from the slot and no ambient flow can "leak" through the buoyant jet if it penetrates the full depth and does not disintegrate into ribbons. However, there may be insufficient turbulence to produce a completely mixed flow field downstream and close to the outfall. Ultimately, there will always be a uniform mixture of jet effluent and ambient flow far downstream from the outfall section.

When the buoyant, slot jet cannot entrain all the oncoming flow while maintaining the free buoyant jet flow pattern, the jet breaks up and efficient mixing takes place. For the purpose of this study we will call such a situation forced entrainment.

One way to achieve well-mixed conditions is by using an efficient diffuser that ensures a high degree of initial jet mixing. Hence, it is of interest to know in some detail how the over-all mixing varies with the design and operation of a diffuser. The slot arrangement used in the present investigation is a simple but well-defined diffuser.

The graphical representation of observed flow regimes is complicated by the fact that the general flow situation – a buoyant slot jet in ambient flow – is characterized by four dimensionless parameters. However, we may shorten the list of independent variables selected on page 3 to define the problem by omitting q, the volume flux from the source. It is the initial flux of momentum and buoyancy that significantly affects the dynamics of the present flow phenomenon, not the mass or volume flux from the source. Hence, the new list of independent variables is as follows:

For the source:

kinematic momentum flux $m = u_j^2 B$

kinematic buoyancy flux $b = \frac{\Delta\rho}{\rho} g u_j B$

angle of injection θ

and for the ambient flow:

velocity u_a

depth H

The flow problem is now described by three dimensionless numbers chosen as

1. a source Froude number

$$F = \frac{u_a^3}{b}$$

2. a momentum flux ratio

$$\frac{V}{k} = \frac{u_a^2 H}{m} = \frac{u_a^2 H}{u_j^2 B}$$

3. the angle of injection, θ

Hence, by keeping θ constant we may conveniently plot the experimental data in a F vs. $\frac{V}{k}$ graph. F expresses the relative effect of buoyancy flux from the source on the process of diffusion and $\frac{V}{k}$ measures the ratio of momentum flux of the ambient flow and the source.

Neither the simple plume (buoyancy source) nor the simple jet (momentum source) has any characteristic length. However, a buoyant jet has a typical length characterizing the source which we may define as $m/b^{\frac{2}{3}}$. Hence, as an alternative parameter to the momentum flux ratio we can formulate a dimensionless number P equal to the ratio between the flow depth and this characteristic source length

$$P = \frac{H}{m/b^{\frac{2}{3}}} = F^{-\frac{2}{3}} \frac{V}{k} \qquad (44)$$

P is of interest because it does not include the velocity of the ambient flow. It is a parameter scaling the size of the flow phenomenon relative to the flow depth. For $P > P_o$ we may consider the depth so large that in a region close to the source the free surface has no effect, and the flow domain may be regarded as semi-infinite. *

Fig. 19 is a graphical representation of possible flow regimes. The general flow situation is in the center of the graph. It is surrounded by the limiting cases. In the upper right corner of the graph, input of buoyancy and momentum from the source can be considered negligible. The diffusion is then due to ambient turbulence only.

V-3 Observed Flow Regimes

Experiments were conducted for two cases: $\theta = 0^o$, a horizontal, buoyant jet directed downstream; and $\theta = 90^o$, a buoyant jet issued vertically. The results of these two sets of experiments will be discussed separately.

A buoyant slot jet in a uniform, coflowing stream ($\theta = 0^o$).

The injector device for the buoyant slot jet did not penetrate deeper than about 2 cm into the ambient flow. Although the outfall structure in the experiments may not have induced critical flow as illustrated by Fig. 14a, nevertheless a critical flow section must occur somewhere for cases with an upstream wedge. From a practical standpoint, possible penetration of jet effluent upstream of the outfall section is of interest as well as the over-all mixing as related to the design and operation of the diffuser.

---

* Large P-values also indicate a source of predominant buoyancy flux. In this case the only remaining important parameter is F.

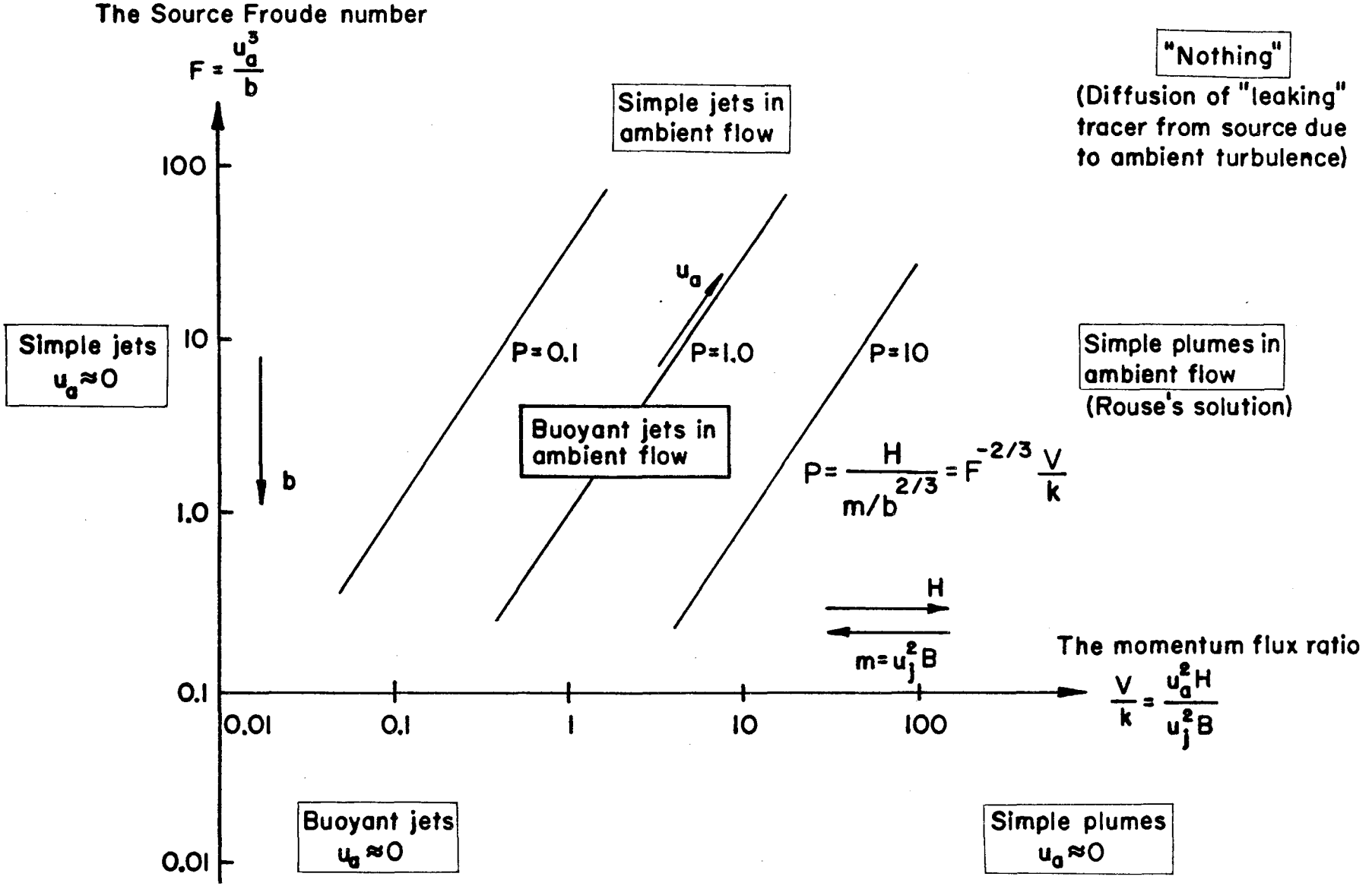

Fig. 19 Graphical representation of flow regimes keeping θ = constant. The general flow situation in the center of the graph is surrounded by the limiting cases. The parameter P is the ratio between the flow depth H and a characteristic length $m/b^{\frac{3}{2}}$ of the source.

It was found to be convenient to relate the formation of a surface wedge to a reference section downstream from the outfall as indicated by Figs. 15 and 16. A surface wedge established at the reference station – here called a subcritical situation – may penetrate upstream from the diffuser. If the jet is swept downstream when reaching the surface at the reference section – here called a supercritical situation – then there will be no jet effluent upstream from the diffuser section. A critical situation corresponds to the case of an incipient surface wedge at the reference section.

Altogether, seventy-three experiments were conducted with a horizontal slot jet. The experiments covered a wide range of both the Froude number F and the momentum flux ratio $\frac{V}{k}$. By observation of the diffusion of the dyed jet effluent, twenty-one of these runs, listed in Table 2, were classified as representing critical flow situations with respect to upstream intrusion of the jet fluid relative to a reference section. Those flow situations that could maintain a free buoyant jet flow pattern are listed in Table 3; Fig. 9 with $u_a \to 0$ is an extreme case illustrating this situation. The data of Tables 2 and 3 are plotted in a F vs. $\frac{V}{K}$ graph in Fig. 20.

To summarize the result, the experimental data have revealed that the gross Froude number F is the important parameter determining the flow regimes. Critical conditions with respect to upstream intrusion of jet effluent related to a reference section downstream of the outfall were observed when F was of the order of unity. The surface wedge is then expelled from the reference section – clearly expelled from the outfall section. Those flow situations that could maintain a free jet or plume-like flow pattern all satisfied the condition $F < 0.2$ in the range

Table 2. Observed critical flow situations for a horizontal slot jet.
(The surface wedge is expelled from the reference section - see Fig. 15)

RUN	$u_a \cdot 10^3$ m/s	$\frac{\Delta\rho}{\rho} \cdot 10^3$	$q \cdot 10^5$ m^2/s	$B \cdot 10^3$ m	H m	F	V	k
5	24	9.2	14.0	1.6	0.50	1.09	86	4
6	26	8.3	30.0	1.6	0.50	0.72	43	8
8	19	6.6	14.0	1.6	0.50	0.76	68	5
12	21	20.0	7.0	1.6	0.50	0.68	150	2
17 c	22	25.2	7.5	1.6	0.50	0.57	147	2
18	60	26.8	62.2	0.75	0.50	1.30	48	14
19	45	16.8	39.0	0.75	0.50	1.42	63	12
20	39	16.8	42.6	0.75	0.50	0.85	46	15
27	48	35.0	32.6	1.2	0.46	0.99	68	6
32	34	35.0	10.7	0.2 *	0.46	1.07	146	16
35	44	35.0	30.0	0.2 *	0.46	0.83	67	34
38	52	35.0	26.6	0.2 *	0.46	1.54	90	26
42	39	47.0	14.7	0.2 *	0.46	0.88	122	19
46	30	20.0	14.7	0.2 *	0.46	0.94	94	24
48	15	20.0	2.2	0.06 *	0.46	0.78	318	24
54 **	15	50.0	1.0	0.2 *	0.46	0.69	690	3
63	46	7.0	120	1.2	0.46	1.18	18	22
67	48	4.3	210	1.2	0.46	1.13	11	36
68	55	4.3	253	1.2	0.46	1.53	10	38
69	45	4.3	213	1.2	0.46	1.02	10	39
71	36	16.0	33.3	1.2	0.46	0.90	50	8

* Equivalent B-value; the slot was replaced by a row of small, closely-spaced ports.

** Not plotted in Fig. 20.

Table 3. Test runs for a horizontal slot jet with free buoyant jet flow pattern observed (cf. Fig. 9).

RUN	$u_a \cdot 10^3$ m/s	$\frac{\Delta\rho}{\rho} \cdot 10^3$	$q \cdot 10^5$ m^2/s	$B \cdot 10^3$ m	H m	F	V	k
13	21	20	23.7	1.6	0.50	0.20	44	8
17 d	22	25.2	20.8	1.6	0.50	0.21	53	6
22 **	11	35.0	23.3	1.2	0.46	0.01	22	17
23 **	11	35.0	12.0	1.2	0.46	0.02	42	9
24	15	35.0	8.0	1.2	0.46	0.12	86	4
29	20	35.0	16.7	0.2*	0.46	0.17	55	42
30 **	9	35.0	10.6	0.2*	0.46	0.02	39	59
40 **	8	47.0	10.0	0.2*	0.46	0.01	37	63
44	15	20.0	10.0	0.2*	0.46	0.17	69	33
51	15	20.0	11.3	1.2	0.46	0.15	61	6
52	10	50.0	3.1	0.2*	0.46	0.06	149	15
53	10	50.0	2.2	0.2*	0.46	0.09	210	11

* Equivalent B-value; the slot was replaced by a row of small, closely-spaced ports.

** Not plotted in Fig. 20.

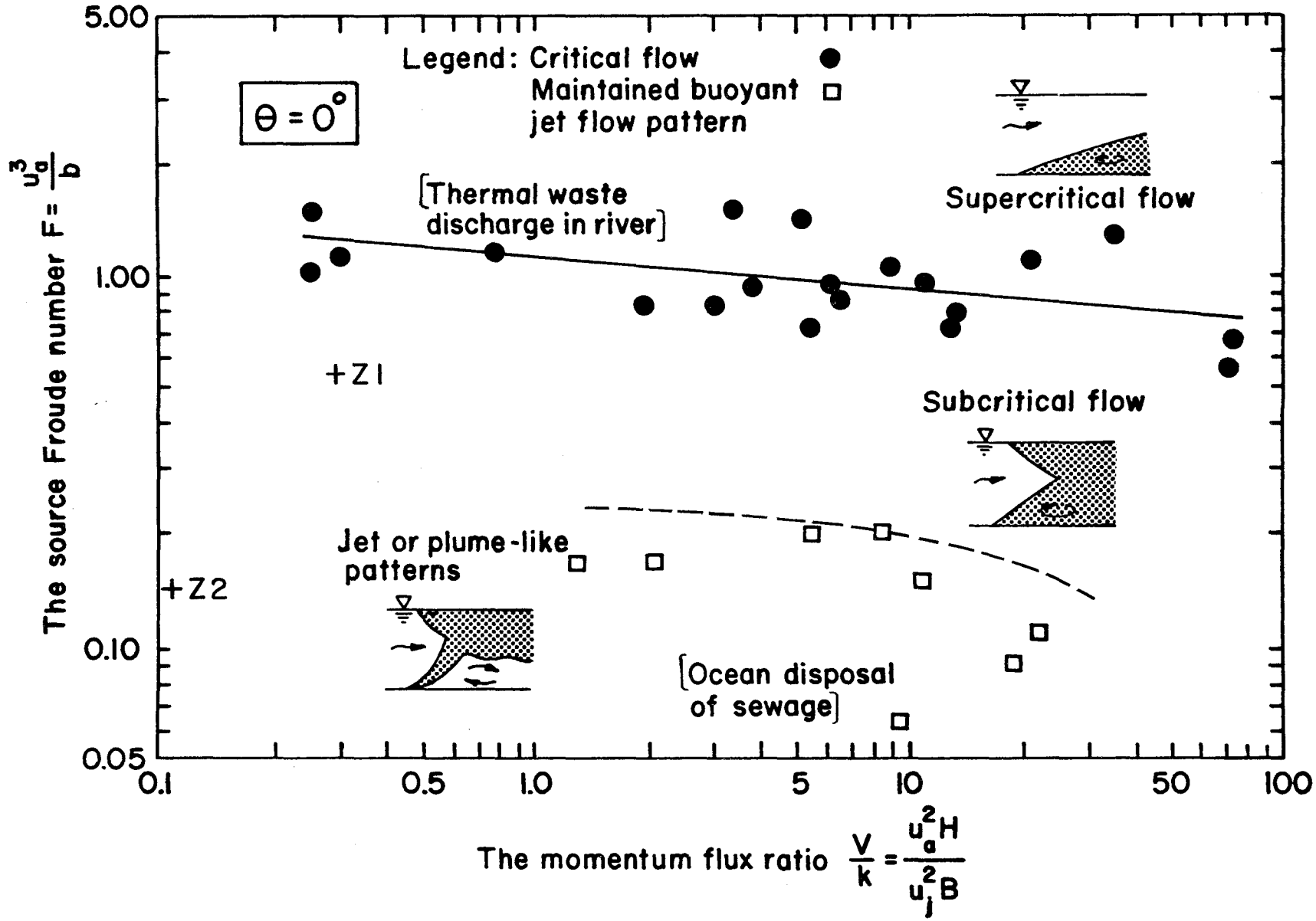

Fig. 20 Observed flow regimes for a horizontal buoyant slot jet in a co-flowing stream. Critical flow defined as the situation when the formation of a surface wedge is incipient at the reference section. (Critical flow, see Fig. 15; subcritical flow, see Fig. 16; jet or plume-like patterns, see Fig. 9.)

of $\frac{V}{k}$ covered by the experiments. As indicated in Fig. 20 there is in these cases a tendency for large-scale recirculation downstream of the blocking slot jet. Whether jet effluent will be recirculated or not depends on the controlling downstream conditions. The mixing is most efficient close to the source when the jet flow pattern breaks up (forced entrainment), which seems to occur when F exceeds a value of about 0.2.

The location of the reference section relative to the outfall varies with the momentum flux ratio $\frac{V}{k}$. Otherwise, $\frac{V}{k}$ is not an especially significant parameter describing the flow regimes of a horizontal slot jet in a flowing environment.

A vertical buoyant slot jet in a uniform cross flow ($\theta = 90^{o}$).

Twenty-eight experiments were conducted with a vertical slot injecting heavy salt solutions downward into the flume flow. The test data are listed in Table 4. A graphical representation of the experimental results are given in Fig. 21. The flow situation is more complex when the buoyant jet is issued vertically than when it is directed horizontally. However in both cases observed, flow regimes agree with what is qualitatively predicted by Fig. 19.

Critical condition with respect to upstream intrusion of jet effluent occurs for F of the order of 0.5 or less for small or moderate values of the momentum flux ratio $\frac{V}{k}$. As $\frac{V}{k}$ increases (the effect of initial flux of momentum diminishes) critical conditions tend to be described by F-values close to unity just as for the case of $\theta = 0^{o}$.

A surface wedge deflected upstream – Fig. 21 – was observed when the momentum flux ratio was small. Similarly, areas in the graph of Fig. 21 can be distinguished where jet- or plume-like flow patterns from the slot are maintained.

Table 4. Experimental data for a vertical buoyant slot jet in a uniform cross-flow.

RUN	$u_a \cdot 10^3$ m/s	$\frac{\Delta\rho}{\rho} \cdot 10^3$	$q \cdot 10^5$ m^2/s	$B \cdot 10^3$ m	H m	F	V	k	$\frac{V}{k}$	Sym.
70	20	41.5	3.0	1.2	0.46	0.66	306	1.3	245	■
71	20	41.5	2.0	1.2	0.46	0.98	460	0.8	548	●
72	13	41.5	4.3	1.2	0.46	0.13	140	2.8	50	■
73	13	24.0	14.7	1.2	0.46	0.06	41	9.4	4.4	□
74	21	24.0	14.7	1.2	0.46	0.26	66	5.9	11	□
75	33	24.0	14.7	1.2	0.46	1.04	103	3.7	28	●
76	33	24.0	26.6	1.2	0.46	0.57	57	6.7	8.5	■
77	33	24.0	65.0	1.2	0.46	0.23	23	16	1.4	□
78	17	12.5	14.7	1.2	0.46	0.37	53	7.2	7.4	□
79	27	12.5	14.7	1.2	0.46	1.09	85	4.6	19	●
80	42	12.5	87.0	1.2	0.46	0.69	22	17	1.3	○
81	31	12.5	41.4	1.2	0.46	0.59	34	11	3.1	●
82	21	7.0	14.7	1.2	0.46	0.91	66	5.8	11	●
83	28	7.0	56.0	1.2	0.46	0.57	23	17	1.4	○
84	21	7.0	103	1.2	0.46	0.13	9.4	41	0.2	△
85	40	7.0	40.0	1.2	0.46	2.3	46	8.3	5.5	●
86	29	7.0	36.0	1.2	0.46	0.99	37	10	3.7	●
87	29	7.0	120	1.2	0.46	0.30	11	35	0.3	△
88	20	7.0	14.7	1.2	0.46	0.79	62	6.1	10	●
89	20	7.0	70.0	1.2	0.46	0.17	13	29	0.5	△
90	42	7.0	126	5.0	0.46	0.85	15	6.0	2.5	●
91	42	7.0	260	5.0	0.46	0.41	7.4	12	0.6	△
92	36	7.0	230	5.0	0.46	0.30	7.2	13	10.5	△
93	29	7.0	30.0	5.0	0.46	1.2	44	2.1	21	●
94	29	7.0	173	5.0	0.46	0.21	7.7	12	0.6	△
95	25	20.0	26.7	5.0	0.46	0.30	43	2.1	20	■
96	25	20.0	17.3	5.0	0.46	0.46	67	1.4	48	■
97	25	20.0	6.7	5.0	0.46	1.18	172	0.5	323	●

No intrusion by wedge ○

Wedge Intrusion □

Deflected wedge △

Maintained plume or jet pattern: Unfilled symbols

Forced entrainment: Filled symbols

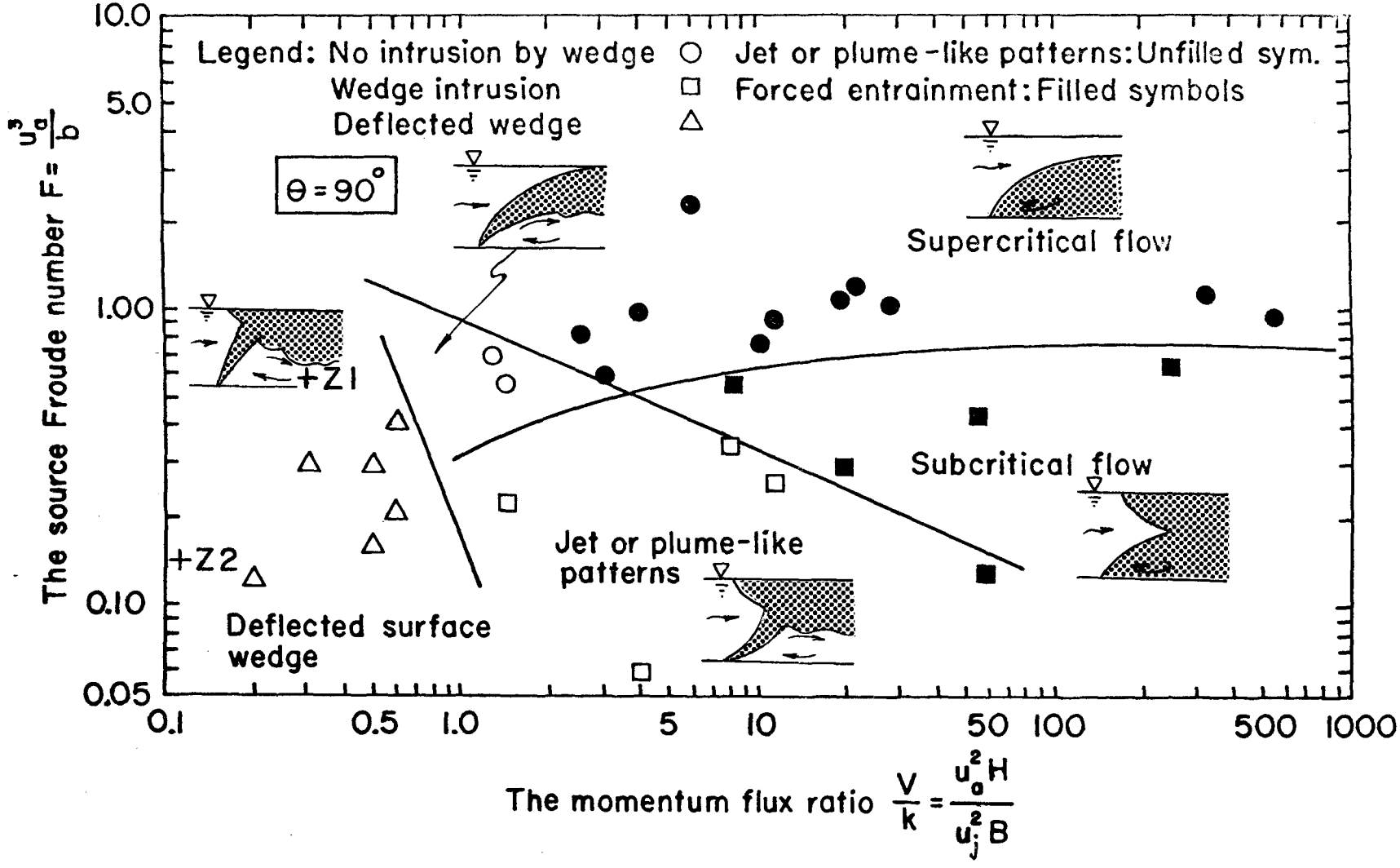

Fig. 21 Observed flow regimes for a vertical, buoyant slot jet in a cross stream. Forced entrainment is defined as a situation where the typical buoyant jet flow pattern breaks up and there is efficient mixing close to the source. (Deflected wedge, see Fig. 17, jet or plume-like patterns, supercritical flow, see Fig. 18.)

It was observed for both the horizontal and vertical slot jets that mixing between the jet effluent and the oncoming flow was very efficient when F was of the order of unity, that is, in a critical flow situation with respect to upstream intrusion of jet effluent; see Section V-5 for the result of some conductivity measurements in the region downstream of the outfall.

V-4 Gravitational Diffusion in Two-Dimensional Flow

Conductivity measurements were made in the 2-foot wide flume to study the mixing downstream from the buoyant slot jet. Before analyzing the result of these measurements we have to consider more in detail the case of gravitational diffusion from a boundary source in two-dimensional flow. This problem – number 8 of the limiting cases listed on page 6 – was, as mentioned previously, subjected to an early study by Rouse (1947). Although gravitational diffusion may apply to many environmental phenomena (such as mixing of thermal waste water), this study of Rouse was focused on a very special problem. During the Second World War, gasoline burners at ground level producing convection currents down-wind from the source were used as an important means of dispersing fog over airfields. The purpose of the investigation was to find the required input of heat as a function of burner location and cross-wind velocity.

Dimensional arguments

We will now use dimensional arguments to derive the main relations describing gravitational diffusion from a boundary source in two-dimensional flow. Fig. 22 is a sketch of the flow situation.

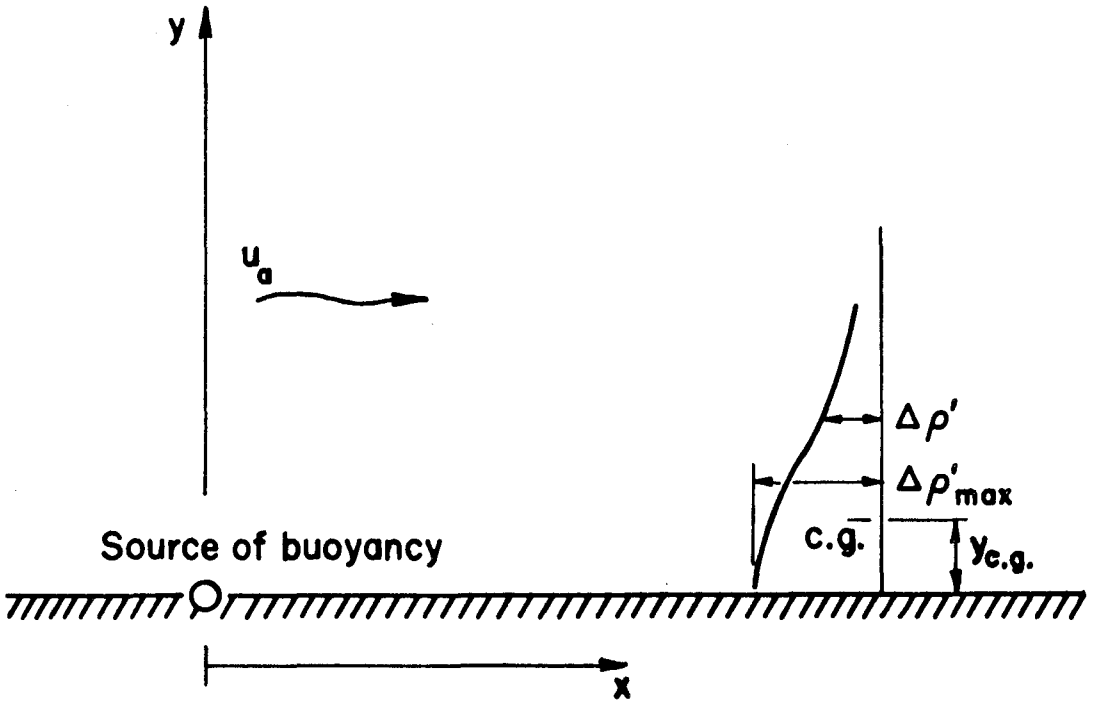

Fig. 22 Definition sketch of gravitational diffusion from a boundary source in two-dimensional flow.

Consider a steady line-source of buoyancy at right angles to a steady horizontal flow. $\Delta\rho'$ is a local value of the density deficit produced by the input of buoyancy and ρ is a reference density chosen as that of the ambient flow. If boundary layer effects are negligible we may assume the ambient velocity to be a constant and equal to u_a at all levels above the rigid boundary. Restricting the study to the case of fully turbulent conditions, we may omit the effect of viscosity and we are left with the following variables characterizing the process of gravitational diffusion in a steady state situation:

$\frac{\Delta\rho'}{\rho} g$	local apparent gravity (function of x, y)
u_a	ambient velocity (constant)
b	buoyancy flux from source (kinematic)

x longitudinal distance from source

y vertical distance from boundary

An equation for the conservation of buoyancy flux defines b

$$b = \int_0^\infty u_a \frac{\Delta\rho'}{\rho} g \, dy = \text{constant} \tag{45}$$

Hence, from dimensional considerations the following relation should describe the distribution of weight deficiency downstream from the buoyancy source:

$$\frac{\Delta\rho'}{\rho} g \frac{x}{u_a^2} = f\left(\frac{y}{x}, F\right) \tag{46}$$

where $F = \frac{u_a^3}{b}$ is the gross Froude number which previously was found to be the dimensionless flow parameter characterizing this limiting case. To arrive at Eq. (46) the only restrictions imposed were the assumptions of the existence of a steady-state solution and fully turbulent conditions.

However, one interesting solution to the problem is accessible if we make the additional assumption that three of the variables listed above (u_a, b and x) are "kinematically" related to each other – they merely describe the rate at which buoyancy is added to each element of fluid passing over the source if there is no net longitudinal circulation or mixing. Hence, a new, shorter list of variables is as follows:

$$\frac{\Delta\rho'}{\rho} g$$

u_a, b, x $\longrightarrow$ $\frac{b}{u_a}$, $t = \frac{x}{u_a}$

$\frac{b}{u_a}$ — buoyancy force per unit horizontal area of flow downstream

$t = \frac{x}{u_a}$ — time of travel for an element of fluid

y

and consequently from dimensional consideration we get a new solution of the form

$$\frac{\frac{\Delta\rho'}{\rho} gt}{\sqrt{\frac{b}{u_a}}} = f\left(\frac{y}{t\sqrt{\frac{b}{u_a}}}\right) \tag{47}$$

Eq. (47) implies that the "kinematical approach" provides us with a similarity solution. The weight-deficiency distributions are similar in shape at all successive sections downstream from the source. We may define a local maximum value of the weight-deficiency curve, $\Delta\rho'_{max}$, as indicated in Fig. 22 and we arrive at the following relation:

$$\frac{\Delta\rho'_{max}}{\rho} g \sim \frac{\sqrt{\frac{b}{u_a}}}{t} = \frac{F^{-\frac{1}{2}} u_a^2}{x} \tag{48}$$

Let $y_{c.g.}$ be the vertical distance from the boundary to the center of gravity of the weight-deficiency distribution – see Fig. 22. Hence, $y_{c.g.}$ is defined by

$$y_{c.g.} = \frac{\int_0^\infty y \frac{\Delta\rho'}{\rho} g \, dy}{\int_0^\infty \frac{\Delta\rho'}{\rho} g \, dy} \tag{49}$$

Write Eq. (49) in normalized form

$$y_{c.g.} = \frac{\int_0^\infty \eta f(\eta) \, d\eta}{\int_0^\infty f(\eta) \, d\eta} t\sqrt{\frac{b}{u_a}} \tag{50}$$

where

$$\eta = \frac{y}{t\sqrt{\frac{b}{u_a}}} \tag{51}$$

Hence,

$$y_{c.g.} \sim t\sqrt{\frac{b}{u_a}} = x F^{-\frac{1}{2}} \tag{52}$$

indicates a linear expansion of the diffusion pattern with distance from the source. Assume a Gaussian profile of the weight-deficiency distribution

$$\frac{\Delta\rho'}{\Delta\rho'_{max}} = e^{-\frac{y^2}{2\sigma^2}} \tag{53}$$

where σ^2 is the second moment of this distribution function about y = 0. Therefore,

$$\sigma = \sqrt{\frac{\pi}{2}}\, y_{c.g.} \tag{54}$$

Eq. (47) may now be written

$$\frac{\Delta\rho'}{\rho} g \frac{x}{u_a^2 F^{\frac{1}{2}}} = C_1 \cdot e^{-C_2 \frac{y^2}{x^2}} F \tag{55}$$

C_1 and C_2 are constants one of which may be eliminated by putting Eq. (55) into Eq. (45). This gives us

$$C_1 = \frac{2}{\sqrt{\pi}} C; \quad C_2 = C^2 \quad \text{and}$$

$$\frac{\Delta\rho'}{\rho} g \frac{x F^{\frac{1}{2}}}{u_a^2} = \frac{2}{\sqrt{\pi}} C \cdot e^{-(C\frac{y}{x})^2} F \tag{56}$$

where the constant C has to be evaluated from the result of experiments.

The general solution of the problem as given by Eq. (46) has the advantage that it indicates that there is a certain range of validity of Eq. (56) presumably given by

$$F > F_o \tag{57}$$

If the buoyancy is too strong and F is less than such a critical F_o-value, large-scale instability may develop affecting the main flow field; the plume will separate from the boundary and the "kinematical coupling" between u_a, b, and x does not hold any more. It is also predicted that $F_o > 1$ because no wedge is permissible. From a few limited experiments (below) it appears that F_o might be of the order of 2.

Rouse's solution

Rouse analyzed the problem of gravitational diffusion by using two related equations, one of work-energy and one describing the vertical diffusion of weight-deficiency. He assumed that the rate at which work is done by buoyant forces equals the rate of gain of turbulent energy and he adopted a mixing-length approach to solve his equations. Rouse introduced an error in his calculations by putting $\sigma = y_{c.g.}$ (compare Eq. (54)); however, by repeatedly doing so, the errors canceled and his result is still of the principal form given by Eq. (56). By comparing with experimental data obtained in 1943 by the Iowa Institute of Hydraulic Research the constant C of Eq. (56) was evaluated as

$$C = 2.3 \tag{58}$$

and Rouse suggested the following equation to describe two-dimensional gravitational diffusion from a boundary source:

$$\frac{\Delta\rho'}{\rho} g \frac{x F^{\frac{1}{2}}}{u_a^2} = 2.6\, e^{-5.4 \frac{y^2}{x^2}} F \tag{59}$$

Comparison between diffusion of ambient turbulence and gravitational diffusion.

To illustrate the essential difference between diffusion due to ambient turbulence, and that due to gravitational convection, let us derive an equation similar to Eq. (59) but with an assumed constant coefficient of diffusion. The steady state equation for conservation of mass in a two-dimensional flow situation may be reduced to

$$u_a \frac{\partial c}{\partial x} = \frac{\partial}{\partial y}\left(\varepsilon \frac{\partial c}{\partial y}\right) \tag{60}$$

where c is the concentration by volume of a particular tracer element of the source. Eq. (60) expresses a balance between vertical diffusion and horizontal advection. With $t = x/u_a$, the travel time, we get

$$\frac{\partial c}{\partial t} = \frac{\partial}{\partial y}\left(\varepsilon \frac{\partial c}{\partial y}\right) \tag{61}$$

Assume that a proper description of the mixing can be based on a constant value of ε (not varying with y). Then

$$\frac{\partial c}{\partial t} = \varepsilon \frac{\partial^2 c}{\partial y} \tag{62}$$

Eq. (62) is the well-known equation for one-dimensional heat conduction. The solution for point source in semi-infinite domain is; Carslaw and Jaeger (1947)

$$c(y,t) = \frac{A}{\sqrt{4\pi\epsilon t}}\, e^{-y^2/4\epsilon t} \tag{63}$$

The source strength A, is determined from a continuity relation

$$u_a \int_0^\infty c\, dy = q \cdot c_o \tag{64}$$

and

$$A = \frac{2\, q\, c_o}{u_a} \tag{65}$$

This gives the following relation for the concentration distribution

$$\frac{c(x,y)}{c_o} = \frac{q}{\sqrt{\pi\, \epsilon\, x\, u_a}}\, e^{-y^2 u_a/4\epsilon x} \tag{66}$$

Write Eq. (59) in a similar way

$$\frac{c(x,y)}{c_o} = 2.6\, \frac{q\, F^{\frac{1}{2}}}{u_a\, x} \cdot e^{-5.4\, F \left(\frac{y}{x}\right)^2} \tag{67}$$

to stress the differences in the diffusion pattern.*

V-5 Conductivity Measurements

The dissolved salt of the jet fluid not only models the density difference, but it is also a convenient tracer material. Hence, to study the over-all mixing in the region close to the outfall, some conductivity measurements were made in the 2-foot wide flume just as for the experiments in stagnant water. Fig. 23 shows the test sections.

The conductivity probe was mounted on a point gage fixed to a moveable carriage on top of the flume. Conductivity readings were taken at 4-cm depth intervals. Concentration profiles are

---

* See also discussion on page 69.

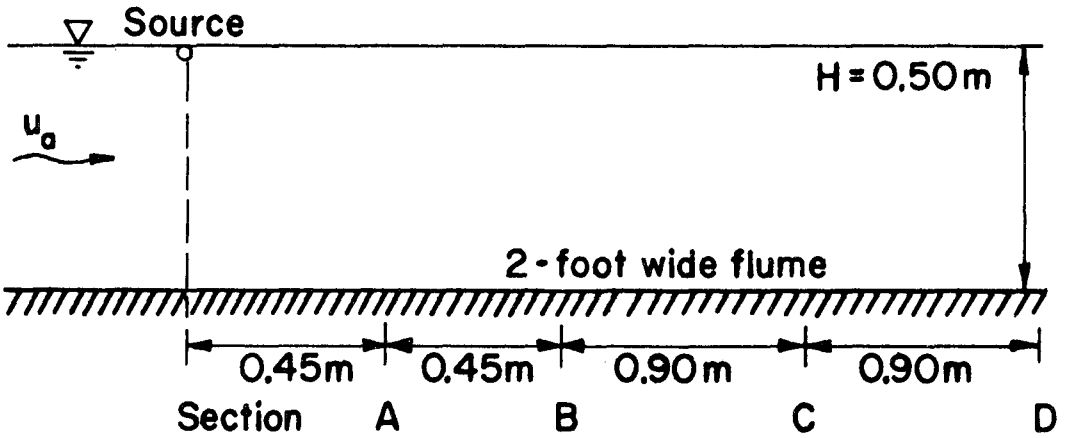

Fig. 23 Test sections used for conductivity measurements in the 2-foot wide flume. Compare also Fig. 10.

available for the first twelve runs with a horizontal buoyant slot jet in flowing ambient water. The results can be used to characterize the flow regimes observed.

A steady-state situation with respect to the flow pattern downstream from the outfall jet is usually rapidly obtained. However, as demonstrated by Figs. 17 and 18 there is, in some experiments, a tendency for large-scale recirculation of fluid downstream from the blocking outfall jet. Depending on the downstream conditions, the recirculated water may ultimately be mixed with jet effluent. It may then take a relatively long time before steady-state is attained, considering the distribution of jet effluent in the flow field. The conductivity measurements were carried out shortly after onset of each experiment.

In a steady-state situation the following relation holds

$$\int_0^H u(c-c_b)dy = q \cdot c_o \qquad (68)$$

where c is the local concentration of the tracer, u is the local velocity in the main flow direction at level y, and c_b is the background concentration of the ambient flow. $q\,c_o$ is the rate of tracer material discharged from the source. Let us define a distribution factor α by

$$\alpha\, u_a\, H(\bar{c}-c_b) = q \cdot c_o \qquad (69)$$

where $\bar{c}$ is the depth-averaged concentration.

$\alpha > 1.0$ indicates positive correlation between velocity and concentration, which may occur at sections where a jet flow pattern is established.

$\alpha < 1.0$ indicates that there are stagnant zones of high concentration (the wedge).

Fig. 24 shows the variation of α with distance from the source for various runs and Fig. 25 some measured concentration profiles.

We can now compare Rouse's solution for gravitational diffusion in a two-dimensional flow field, that is Eq. (59) or Eq. (67), with measured distributions of concentration. Runs 1, 2, and 3 have F-values that appreciably exceed unity (2.8, 5.2 and 9.5 respectively). Although the vertical diffusion was rapid, there was no sign of developing large-scale instability close to the source in these cases. Hence, as the effect of initial flux of momentum on the diffusion was not very significant, (V/k was 198, 160 and 377 respectively for these three runs), the measured concentration profiles should match Eq. (67) pretty well. Fig. 26, a graphical representation of Rouse's solution and the present experimental data, shows that this is the case. There is a considerable scatter of the points; however, this was also experienced by Rouse in similar experiments.

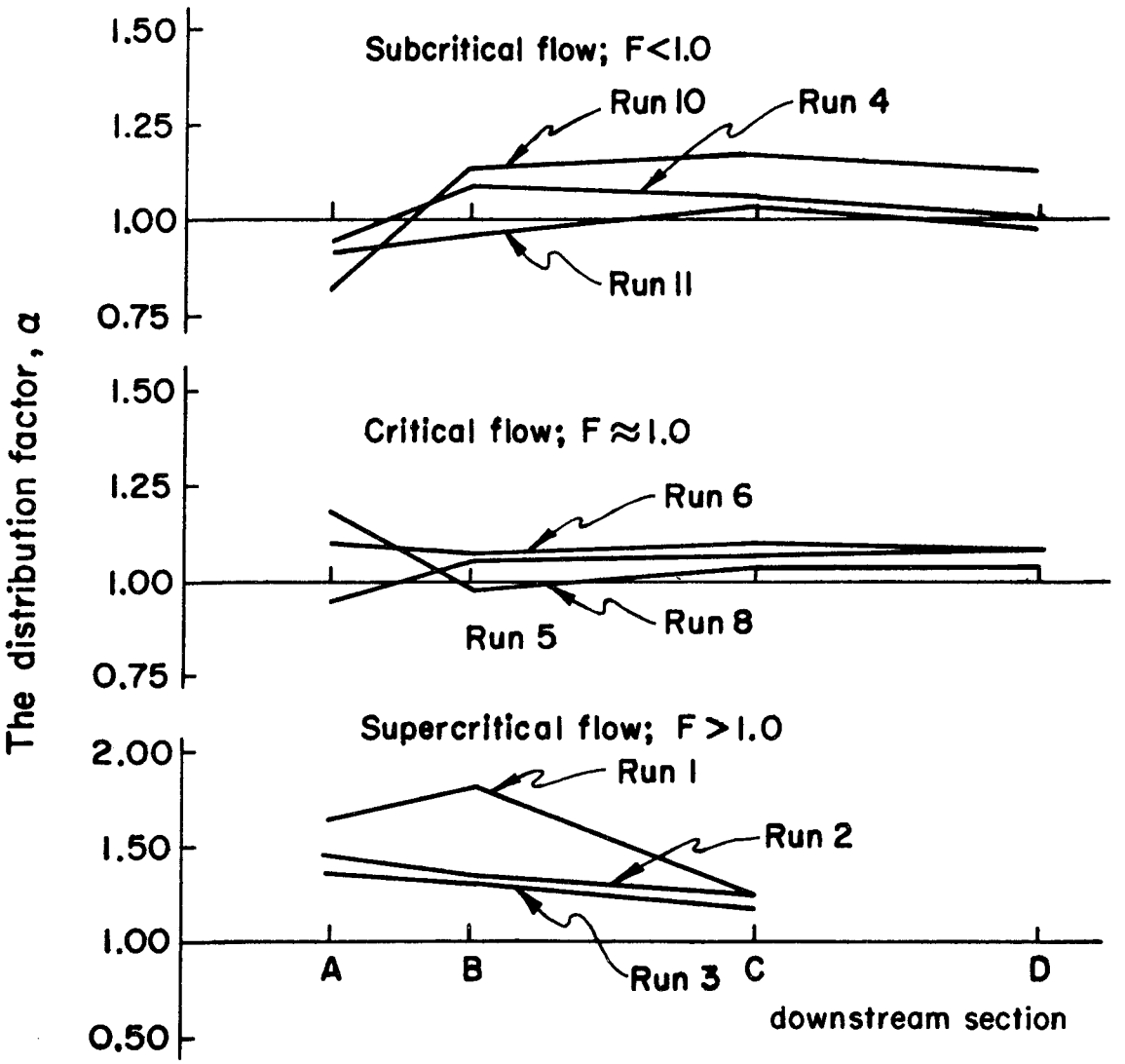

Fig. 24 The distribution factor, α, for experiments with a horizontal, buoyant slot jet.

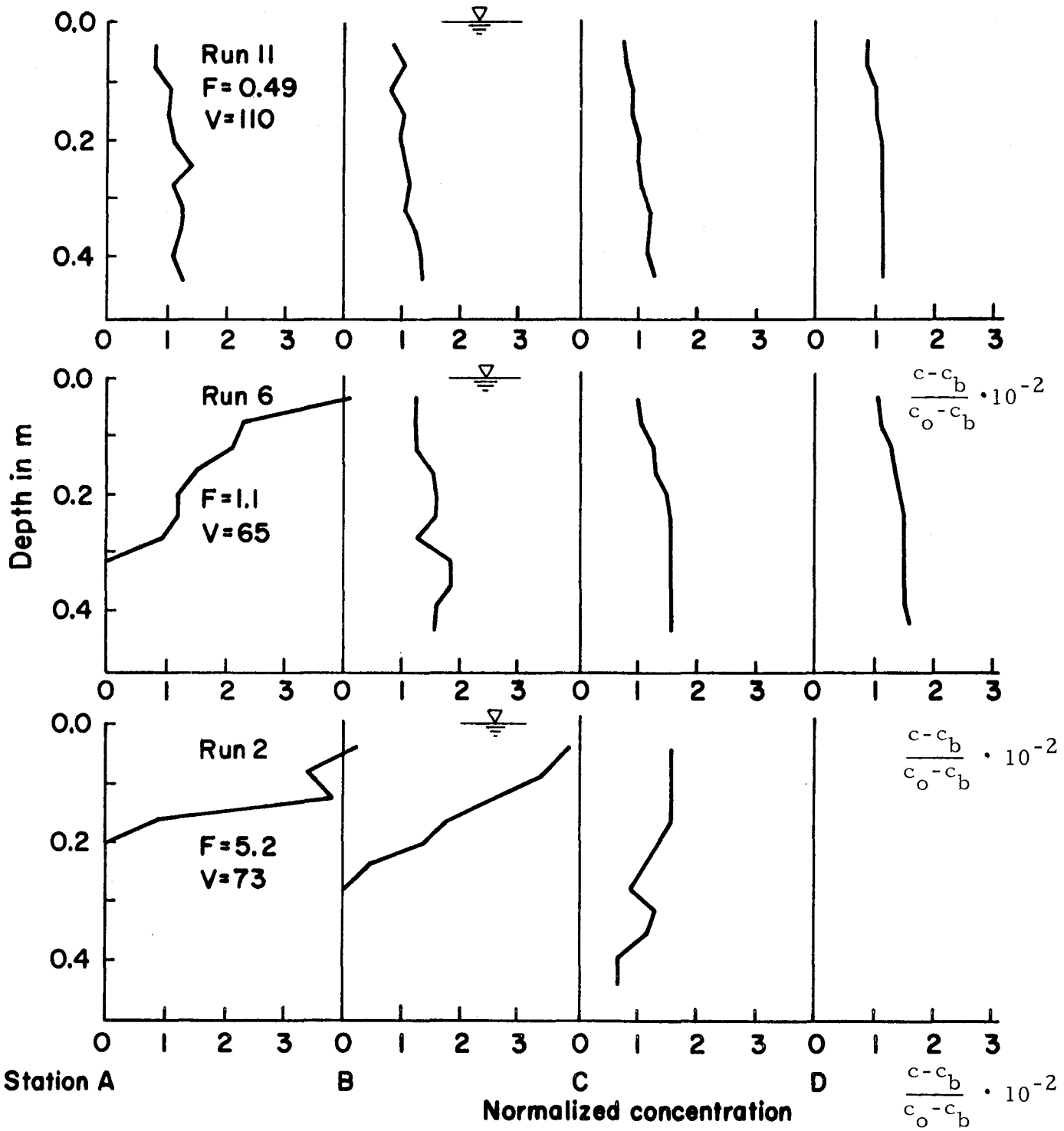

Fig. 25 Concentration profiles for three typical runs with a horizontal buoyant slot jet in a co-flowing stream. The source is at the surface 0.45 m upstream of Section A (see Fig. 23).

Consider, for the purpose of comparison, a two-dimensional shear flow field. A mean value of the coefficient for vertical diffusion of momentum is

$$\epsilon = \frac{1}{15} H u_* \tag{70}$$

where u_* is the friction velocity. A typical wall roughness may give us the following velocity ratio

$$\frac{u_a}{u_*} = 20 \tag{71}$$

Hence, in normalized form we may write a representative diffusivity as

$$\frac{\epsilon}{H u_a} = \frac{1}{300} \tag{72}$$

In case of gravitational diffusion a corresponding value of the diffusivity is evaluated from

$$\epsilon = \frac{1}{2}\frac{d\sigma^2}{dt} = \frac{1}{2} u_a \frac{d\sigma^2}{dx} \tag{73}$$

Eq. (67) gives

$$\epsilon = \frac{1}{2} u_a \frac{d}{dx}\left(\frac{x^2}{10.8F}\right) \tag{74}$$

and

$$\frac{\epsilon}{u_a H} = \frac{x}{H}\frac{1}{10.8F} \tag{75}$$

The coefficient of diffusion is now a linear function of the distance from the source. Hence, compared to diffusion of momentum in shear flow, gravitational diffusion is a very efficient process. *

---

* For example, if F=10, the relative diffusivity in case of gravitational diffusion may be 30 times the relative rate of diffusion of momentum in open-channel flow at a distance 10 flow depths downstream of the source. At a section 100 flow depths downstream from the source this ratio is increased to 300. The differences in diffusion rates become more pronounced for smaller F-values.

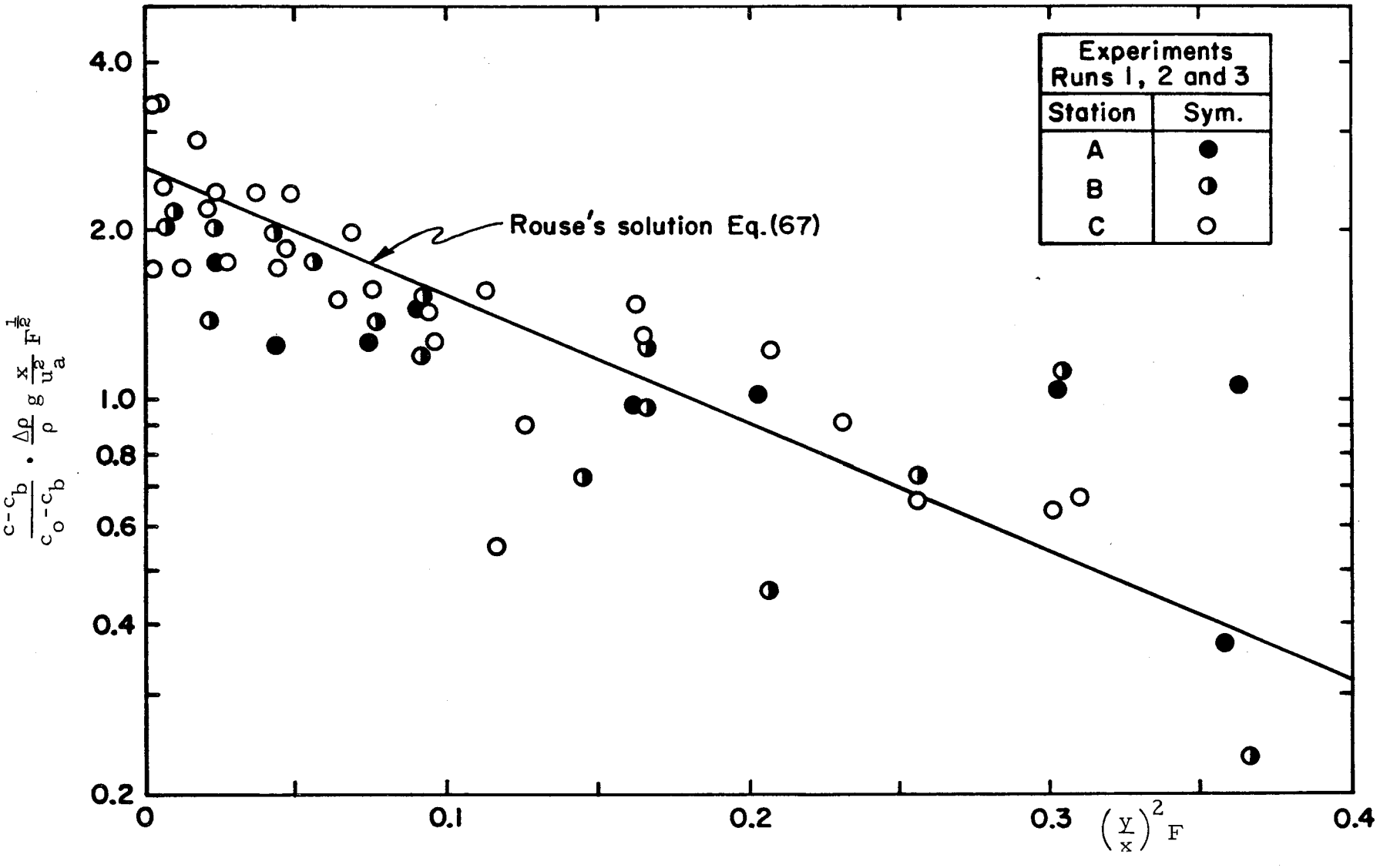

Fig. 26 Rouse's solution of gravitational diffusion from a boundary source in two-dimensional flow compared with experimental data.

V-6 Model Studies on Thermal Diffusion

Hydraulic models have been employed for many years as an important tool in the solution of thermal pollution problems. Basic studies of thermally stratified flow related to the proper design of cooling water arrangements have been conducted by Bata (1957). Recent investigations by Harleman and his colleagues at M. I. T. are valuable contributions to our understanding of the fundamental mechanisms of thermal diffusion.

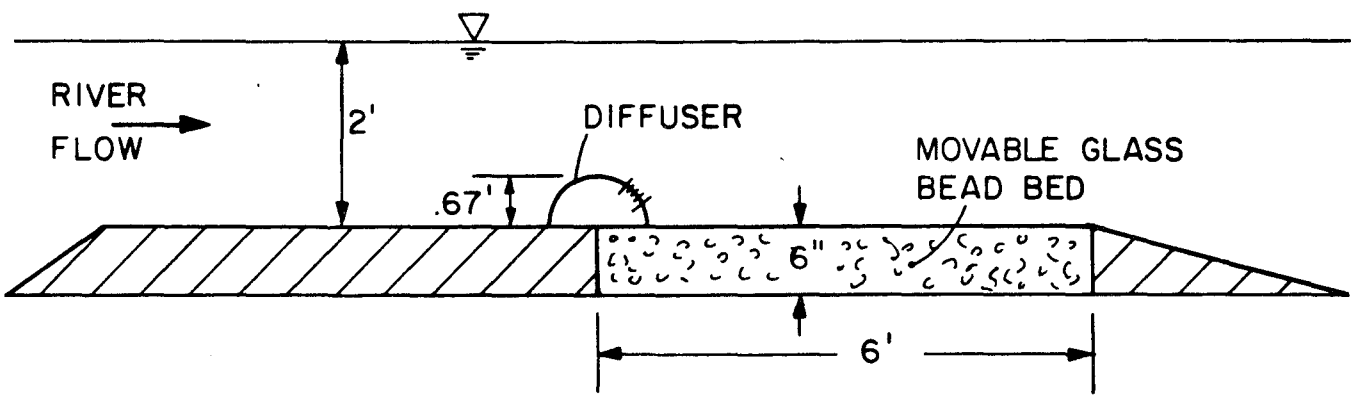

Fig. 27 The sectional model of the cooling water diffuser for Browns Ferry Nuclear Power Station was built to a length scale ratio of 1:15 and placed in a 90-ft long flume. Figure shows scour model.

Of interest for comparison with the result of the present findings is a study, with a two-dimensional undistorted model, of a section of the diffuser pipe for Browns Ferry Nuclear Power Plant (Harleman, Curtis and Hall (1968)). The diffuser is expected to produce a uniform downstream temperature field. The design and operation of this diffuser is based on the mixing and entrainment of a larger number of small jets

of heated condenser water. The jet ports of the diffuser pipe are closely spaced and located in several horizontal rows on the downstream quadrant of the diffuser, see Figs. 27 and 28.

The experiments confirmed that a critical depth occurs in the lower layer as it flows over the top of the diffuser. The most important conclusion, however, was that complete mixing is achieved a relatively short distance downstream from the diffuser. There was no significant difference in the over-all mixing when the port size or port spacing were varied. The only important difference was with respect to the jet angle.

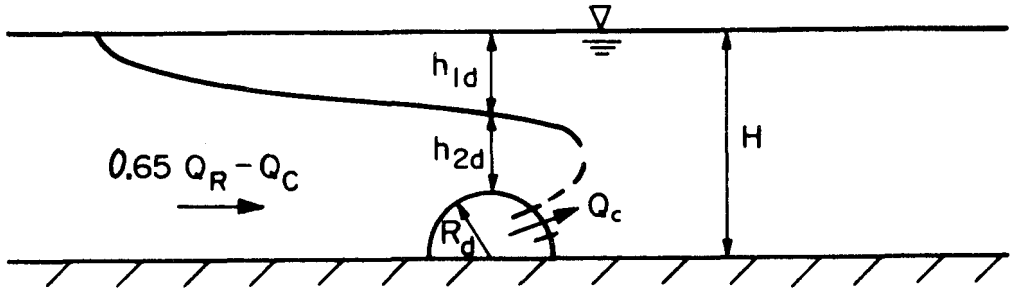

Fig. 28 Definition sketch of flow situation for the diffuser arrangement of Browns Ferry Nuclear Power Station. About 65% of the river flow is through the main channel occupying the diffuser.

A larger distance was required to obtain complete mixing for the case in which the diffuser jets discharged horizontally. Fig. 29 shows the result of two typical experiments with the diffuser design chosen for the prototype. The jet angles relative to the river bed varied from 24° to 41°. The isotherms are drawn for steady-state river flows. With the definitions of Fig. 28 we can now evaluate the source Froude number F at the diffuser section.

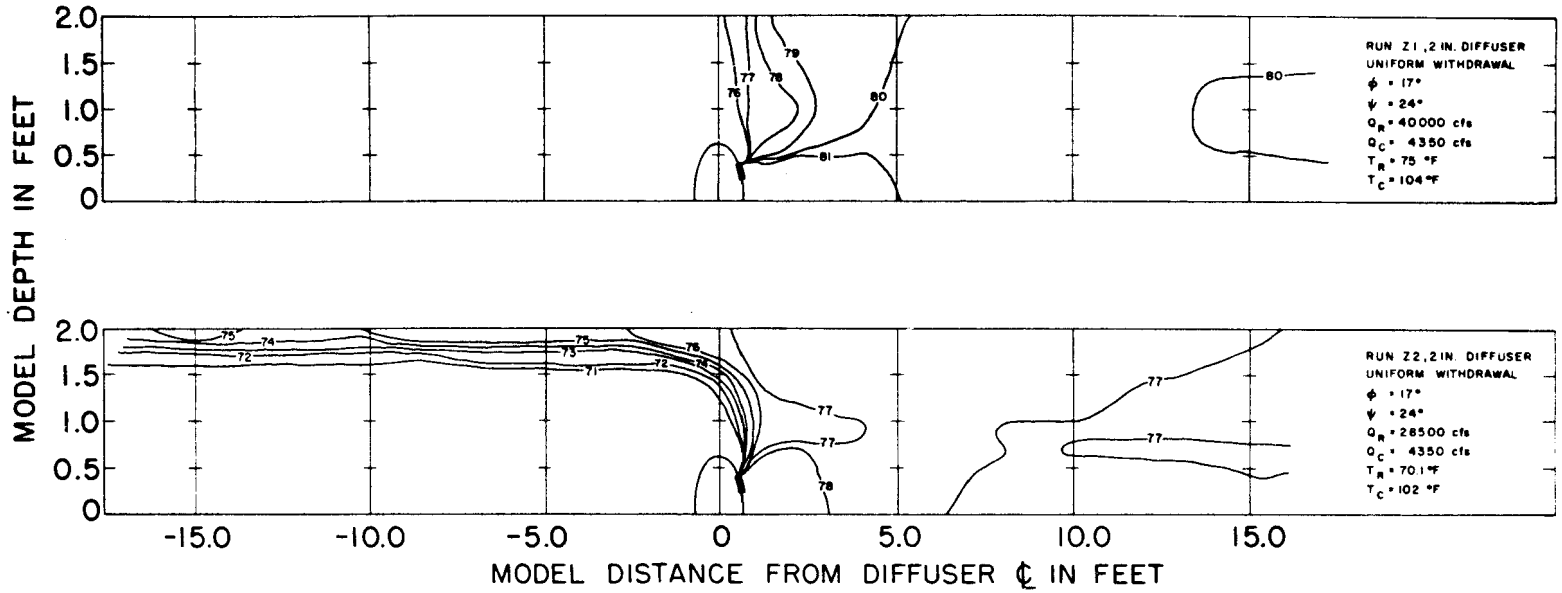

Fig. 29 Isotherms drawn for two model runs for the Browns Ferry Nuclear Power Plant. The river flow is from the left. From Harleman, Curtis and Hall (1968).

The condenser water discharge per unit diffuser length is equal to

$$q = \frac{Q_c}{L}$$

where L is the actual length of the diffuser pipe. About 65 per cent of the river flow is through the main channel occupying the outfall structure (L = 1800 ft and H = 30 ft). Hence, the oncoming flow is

$$[0.65\,Q_R - Q_c]/L$$

per unit width where Q_R is the total river flow. A source Froude number F related to the diffuser section may now be written

$$F = \frac{\left[0.65\,Q_R - Q_c\right]^3}{Q_c L^2 \frac{\Delta\rho}{\rho} g \left(H - R_d\right)^3} \tag{76}$$

$\frac{\Delta\rho}{\rho}$ is, as before, the relative density deficit of the condenser water and R_d is the radius of the diffuser (see Fig. 28). $\frac{\Delta\rho}{\rho}$ is calculated to be $5.0 \cdot 10^{-3}$ for the upper run (Z1) of Fig. 29 and $5.5 \cdot 10^{-3}$ for the lower run (Z2).

Similarly, the momentum flux ratio $\frac{V}{k}$ related to the diffuser section can be estimated

$$\frac{V}{k} = \frac{\left[0.65\,Q_R - Q_c\right]^2 A_j}{Q_c^2 (H - R_d) L} \tag{77}$$

where A_j is an equivalent jet slot area of the diffuser. In the final design the diffuser is provided with approximately twelve ports per foot of the diffuser length. The ports were 2-inches (5.1 cm) in diameter and they were distributed along the diffuser pipe in an arrangement as described above. When evaluating A_j, the jet contraction (discharge

coefficient) was assumed to be 0.6 on an average for the ports (see the report on the hydraulic design of the multiport diffuser, Vigander, Elder and Brooks (1970)).

Comparison with present study

The parameters F and $\frac{V}{k}$ are calculated for the two experimental runs shown in Fig. 29, and the values are listed in Table 5. From the table it follows that observed and predicted flow regimes are in reasonable agreement – the special diffuser arrangement used in the model study does not allow for an exact comparison with the present buoyant slot jet experiments. It is also of interest to note, from the result of the model study, that there is almost horizontal, thermal stratification above the diffuser when the flow is critical (Fig. 29). The result of the present investigation also indicates very efficient mixing – relatively independent of the initial jet mixing characteristics – in a flow situation when the formation of a surface wedge is incipient at the reference section (in this case the outfall section).

Table 5. Two experiments from the Browns Ferry Nuclear Power Plant study compared with result of present buoyant slot jet experiments.

Run	The source Froude number F	The momentum flux ratio V/k	Observed flow	Predicted flow regime from present buoyant slot jet study
Z1 $\theta \sim 32^{\circ}$	0.56	0.2	Critical flow: the wedge is incipient at the reference section (outfall section).	Fig. 20 for $\theta=0^{\circ}$: subcritical. Fig. 21 for $\theta=90^{\circ}$: supercritical (deflected surface wedge?).
Z2 $\theta \sim 32^{\circ}$	0.14	0.1	Subcritical flow: the wedge penetrated far upstream from the outfall section.	Fig. 20 for $\theta=0^{\circ}$ subcritical (jet-or plume-like pattern). Fig. 21 for $\theta=90^{\circ}$: deflected surface wedge.

CHAPTER VI

CONCLUSIONS

A buoyant slot jet into a stagnant or uniformly flowing environment, as illustrated by the definition sketch of Fig. 1, has been studied. The general flow situation is characterized by four dimensionless numbers chosen as:

1. a source Froude number $F = \frac{u_a^3}{b}$
2. a velocity ratio $k = \frac{u_j}{u_a}$
3. a volume flux ratio $V = \frac{u_a H}{q}$
4. the angle of injection θ

Several limiting cases can be defined where the flow field is described by a reduced number of parameters (see Section II-2 and Fig. 19).

VI-1. A Horizontal Buoyant Slot Jet Into Stagnant Environment

Experimental data obtained from conductivity measurements to determine the centerline dilution of the jet effluent as well as the jet trajectory are in reasonable agreement with existing theories of Abraham (1963) and Fan and Brooks (1969) (see Figs. 6, 7 and 8).

Graphical representations of jet trajectories and centerline dilution are given in which the solution of Abraham collapses into simple curves for all F_j. When plotting the theory of Fan and Brooks

in these graphs, F_j is still a free parameter although the variation with F_j is small, and differences from Abraham's result are minor.

VI-2 A Buoyant Slot Jet Into Uniformly Flowing Environment

1. The flow regime is generally determined by four dimensionless numbers. For small mass flow from the source (the source is then characterized by initial flux of momentum, m, and buoyancy, b, only) the governing flow parameters reduce to (Fig. 19)

1. F

2. $\frac{V}{k} = \frac{u_a^2 H}{u_j^2 B}$ (a momentum flux ratio)

3. θ

2. The experiments show classes of flow regime in Fig. 20 for $\theta = 0^o$ (horizontal buoyant slot jet in co-flowing stream) and in Fig. 21 for $\theta = 90^o$ (a vertical buoyant slot jet in a cross-stream).

3. With respect to upstream intrusion the principal flow regimes are identified as:

a) Supercritical flow (see Fig. 18). The jet flow is swept downstream when reaching the surface.

b) Critical flow (see Fig. 15). The upstream intrusion of the wedge is incipient at the reference section.

c) Subcritical flow (see Fig. 16). A surface wedge penetrates upstream from the reference section.

4. With respect to mixing characteristics, the flow pattern is either:

   a) jet- or plume-like (Fig. 9), or

   b) characterized by forced entrainment defined as the situation when the buoyant jet cannot entrain all the oncoming flow while maintaining the free buoyant jet flow pattern (Fig. 15). The jet then breaks up and efficient mixing takes place close to the source.

5. Gravitational diffusion in two-dimensional flow. For super-critical conditions characterized by

$$\frac{V}{k} \text{ large}$$

$$F > F_o \quad (F_o \text{ may be of the order of two})$$

the over-all mixing resembles that of gravitational diffusion from a boundary source in semi-infinite two-dimensional flow.

Using dimensional argument and a wall-diffusion-layer assumption it was possible to derive

   a) a similarity relation for the vertical weight-deficiency profile downstream from the source (Eq. 47) and

   b) a main relation (Eq. 56) describing the process of gravitational diffusion with one empirical constant. Rouse (1947) suggested an equation (Eq. 59) of the same principal form.

Rouse's solution for gravitational diffusion was compared to measured concentration profiles for some runs with large V/k-values and F > 2. There was good agreement between experimental data and theory.

6. A brief description is given for the thermal diffusion study for the Browns Ferry Nuclear Power Plant in relation to the present regime description. The special diffuser design proposed for the Browns Ferry Nuclear Power Plant does not allow for an exact comparison with the buoyant slot jet experiments of this study. The result of the thermal diffusion study for the multiple diffuser is, however, in qualitative agreement with the present regime description.

VI-3 Practical Applications

Two practical problems of waste water disposal, relevant to the present study, have been emphasized: thermal diffusion of condenser water in a river and sewage disposal to a marine environment (see Section III-2 and Fig. 20).

Thermal diffusion of waste water in a river is governed by both the Froude number F and the momentum flux ratio V/k of the order of unity. It is a diffusion process in a confined region.

Submarine disposal of sewage is characterized by considerably smaller F-values and large V/k-values. It is essentially an unconfined diffusion process.

Multiport diffusers are usually designed to approximate a line source. In case of thermal waste water discharge in a river, the current may then have pronounced dynamic effects on the mixing pattern; however, in the ocean disposal case the current effect is mainly kinematic–the jet trajectories are merely bent downstream.

NOTATIONS

The main symbols used in this study are listed below.

B	jet slot width
b	buoyancy flux from source as defined by Eq. (3)
C	constant
c	local concentration
c_b	background concentration
c_m	centerline concentration
c_o	initial concentration
$\bar{c}$	depth-averaged concentration
D	jet diameter
F	Froude number as defined by Eq. (5)
F_D	Froude number as defined by Eq. (23)
F_j	Froude number as defined by Eq. (7)
F_R	Froude number as defined by Eq. (22)
g	acceleration of gravity
H	depth
k	velocity ratio as defined by Eq. (4)
L	diffuser length
M	kinematic momentum flux
m	kinematic momentum flux from source as defined by Eq. (2)
n	number of ports per unit length of diffuser

NOTATIONS (continued)

Q, q	flow rates
R_{ej}	jet Reynolds number as defined by Eq. (25)
r	radial coordinate
S	dilution
S_m	centerline dilution
s	coordinate along axis of jet
t	nominal half-width of jet or plume
u	velocity
u_a	ambient velocity
u_j	jet velocity
u_*	shear velocity
V	volume flux ratio as defined by Eq. (6)
x, y, z	cartesian coordinates
α	coefficient of entrainment; also distribution factor as defined by Eq. (69)
β	local inclination of jet axis
ρ	reference density
$\Delta\rho$	initial density difference
$\Delta\rho'$	local density difference
ε	coefficient of diffusion
λ	spreading ratio
ν	kinematic viscosity
τ	shear stress
θ	angle of slot jet as defined by Fig. 1

REFERENCES

Abbot, M. B., "On the Spreading of One Fluid Over Another", LaHouille Blanche, 16, No. 6, 1961, pp. 827-846.

Ackers, P., "Modeling of Heated-Water Discharges", in Engineering Aspects of Thermal Pollution, ed. by Vanderbilt University Press, 1969.

Abraham, G., "Jet Diffusion in Stagnant Ambient Fluid", Delft Hydraulics Laboratory, Publ. No. 29, July 1963.

Abraham, G., "The Flow of Round Buoyant Jets Issuing Vertically Into Ambient Fluid Flowing in a Horizontal Direction", 5th International Water Pollution Research Conference, San Francisco, 1970.

Albertson, M. L., et. al., "Diffusion of Submerged Jets", Trans. ASCE, Vol. 115, 1950, pp. 639-664.

Bata, G. L., "Recirculation of Cooling Water in Rivers and Canals", Jour. of Hyd. Div., ASCE, Vol. 83, No. HY3, June 1957, pp. 1265-1 to 1265-27.

Benjamin, T. B., "Gravity Currents and Related Phenomena", Jour. of Fluid Mech., Vol. 31, No. 2, Jan. 1968, pp. 209-248.

Carlshaw, H. H. and Jaeger, J. C., Conduction of Heat in Solids, Oxford University Press, London, 1947.

Cederwall, K., "Hydraulics of Marine Waste Water Disposal", Hydraulics Div., Chalmers Institute of Technology, Report No. 42, 1968.

Fan, L. -N., "Turbulent Buoyant Jets Into Stratified or Flowing Ambient Fluids", W. M. Keck Laboratory, California Institute of Technology, Report No. KH-R-15, July 1967.

Fan, L. -N. and Brooks, N. H., Discussion of "Horizontal Jets in Stagnant Fluid of Other Density", by Gerrit Abraham, Jour. of Hyd. Div., ASCE, Vol. 92, No. HY2, March 1966, pp. 423-429.

Fan, L. -N. and Brooks, N. H., "Numerical Solution of Turbulent Buoyant Jet Problems", W. M. Keck Laboratory, California Institute of Technology, Report No. KH-R-18, Jan. 1969.

Harleman, D. R. F, Hall, L. C. and Curtis, T. G., "Thermal Diffusion of Condenser Water in a River During Steady and Unsteady Flows (with application to the T. V. A. Browns Ferry Nuclear Power Plant)". Hydrodynamics Laboratory, M. I. T., Report No. 111, Sept. 1968.

REFERENCES (continued)

Harleman, D. R. F., "Mechanics of Condenser-Water Discharge from Thermal-Power Plants", in Engineering Aspects of Thermal Pollution, ed. by Vanderbilt University Press, 1969.

Koh, R. C. Y., "Viscous Stratified Flow Toward a Line Sink", W. M. Keck Laboratory, California Institute of Technology, Report No. KH-R-6, 1964.

Liseth, P., "Mixing of Merging Buoyant Jets From a Manifold in Stagnant Receiving Water of Uniform Density", Hydraulic Engineering Laboratory, University of California, Berkeley, Rep. No. HEL 23-1, November 1970.

Morton, B. R., Taylor, G. I., and Turner, J. S., "Turbulent Gravitational Convection from Maintained and Instantaneous Sources", Proc. Roy Soc. London, A 234, 1956, pp. 1-23.

Okoye, J. K., "Characteristics of Transverse Mixing in Open-Channels", W. M. Keck Laboratory, California Institute of Technology, Rep. No. KH-R-23, December 1970

Platten, J. L. and Keffer, J. F., "Entrainment in Deflected Axisymmetric Jets at Various Angles to the Stream", Dept. of Mech. Eng., University of Toronto, Canada, Report UTME-TP6806, June 1968.

Pratte, B. D. and Baines, W. D., "Profiles of the Round Turbulent Jet in a Cross Flow", Jour. of Hyd. Div., ASCE, Vol. 93, HY6, 1967, pp. 53-64.

Rajaratnam, N. and Subramanga, K., "Plane Turbulent Reattached Wall Jets", Jour. of Hyd. Div., ASCE, Vol. 94, HY1, Jan. 1968, pp. 95-112.

Ricou, F. P. and Spalding, D. B., "Measurements of Entrainment by Axisymmetrical Turbulent Jets", Jour. of Fluid Mech., Vol. 11 1961, pp. 21-32.

Rouse, H., "Gravitational Diffusion From a Boundary Source in Two-Dimensional Flow", Jour. of App. Mech., ASME, Sept. 1947, pp. A225-A228.

Rouse, H., Yih, C. S., and Humphreys, H. W., "Gravitational Convection from a Boundary Source", Tellus, Vol. 4, 1952, pp. 201-210.

Rouse, H., "Diffusion in the Lee of a Two-Dimensional Jet", Proc. 9th Cong. of App. Mech., Univ. of Brussels, Vol. 1, 1957, pp. 307-315.

REFERENCES (continued)

Sawyer, R. A., "Two-Dimensional Reattaching Jet Flows Including the Effects of Curvature on Entrainment", Jour. of Fluid Mech., No. 17, Dec. 1963, pp. 481-498.

Stommel, H. and Farmer, H. D., "Control of Salinity in an Estuary by a Transition", Sears Found. Jour. Marine Research, Vol. 12, No. 1, 1953.

Vigander, S., Elder, R. A. and Brooks, N. H., "Internal Hydraulics of Thermal Discharge Diffusers", Jour. of Hydr. Div., Proc. ASCE, Vol. 96, HY2, Feb. 1970, pp. 509-527.